C_2-Symmetric *ansa*-Lanthanidocene Complexes. Synthesis via Silylamine Elimination and β-SiH Agostic Rigidity

Jörg Eppinger, Michael Spiegler, Wolfgang Hieringer, Wolfgang A. Herrmann, and Reiner Anwander*

Contribution from the Anorganisch-chemisches Institut, Technische Universität München, D-85747 Garching, Germany

Received August 4, 1999

Abstract: The synthesis as well as the spectroscopic and structural characterization of a new class of C_2-symmetric, mononuclear metallocene complexes of the lanthanide elements is described. Heteroleptic lanthanidocene silylamide complexes have been obtained ate-complex-free according to silylamine elimination reactions of complexes $Ln[N(SiHMe_2)_2]_3(THF)_x$ ($x = 1$, Ln = Sc; $x = 2$, Ln = Y, La, Nd, Lu) and linked, substituted cyclopentadiene and indene systems. The molecular structure of $[Me_2Si(C_5Me_4)_2]La[N(SiHMe_2)_2]$ (95% isolated yield) has been determined by X-ray crystallography. Brintzinger-type, indenyl-derived metallocene complexes have been isolated in racemic yields as high as 72%. IR and multinuclear NMR spectroscopy (^1H, ^{13}C, ^{29}Si, ^{89}Y) reveals the presence of an unprecedented strong diagostic interaction between the electron-deficient metal centers and the SiH moiety of the bis(dimethylsilyl)amide ligand: SiH stretching vibrations as low as 1759 cm^{-1} and $^1J_{Si,H}$ coupling constants as low as 133 Hz indicate a distinct weakening of the SiH bonding. X-ray structure analyses of the compounds *rac*-$[Me_2Si(2\text{-}Me\text{-}Benz\text{-}Ind)_2]Ln[N(SiHMe_2)_2]$ (Ln = Y, Lu) and *rac*-$[Me_2Si(2\text{-}Me\text{-}C_9H_5)_2]Ln[N(SiHMe_2)_2]$ (Ln = Y, Lu) show that the structural features of both the chelating ancillary ligands and such agostically fused metallacycles depend on the type of the ligand and the size of the metal: bite angles Ω of approximately "U-shaped" *ansa*-ligands as large as 68.2(2)° and Ln−Si and Ln−H contacts as close as 3.028(1) and 2.37(3) Å, respectively, have been detected, the latter forcing very large Si−N−Si angles up to 160.1(2)°. The isolation of reaction intermediates such as $Y[N(SiHMe_2)_2]_3(THF)$ and partly exchanged $[Me_2Si(2\text{-}Me\text{-}4\text{-}Ph\text{-}Ind)_2H]Y[N(SiHMe_2)_2]_2$ provides mechanistic details of this peculiar silylamine elimination reaction. Additionally, the pK_a values of various protonated ligands including new 9-($SiHMe_2$)-fluorene, 3-($SiHMe_2$)-indene, and 3-($SiHMe_2$)-2-Me-indene determined according to the method of Fraser give evidence of a thermodynamically controlled ligand exchange.

Introduction

During the past decade lanthanidocene chemistry developed into a prolific branch of metallocene research.[1] Although the first lanthanidocene complexes, "Cp_2LnR", comprising unsubstituted cyclopentadienyl rings were reported as early as 1963 by Dubeck et al. (Figure 1, **A**),[2] it was the discovery of the lanthanidocene-based "Ziegler−Natta" model which decisively stimulated the development of this class of compounds.[3] Meanwhile, several generations of rare earth metallocene complexes form an integral part of the enantioselective synthesis of both polymers and fine chemicals.[4,5] For example, achiral lanthanidocene complexes of type **B** promote the stereoregular polymerization of functionalized olefins such as acryl esters,[6] while C_1-symmetric derivatives of type **C** selectively catalyze a variety of olefin transformations including the hydroamination/cyclization of α,ω-aminoolefins.[7] C_2-Symmetric yttrocene com-

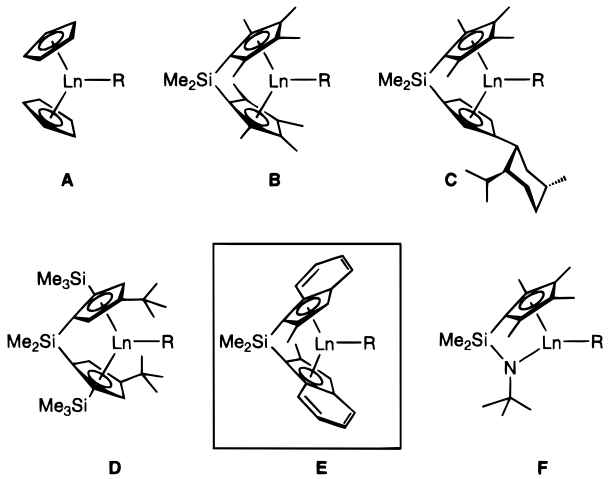

Figure 1. Various generations of lanthanidocene complexes.

(1) (a) Burger, B. J.; Cotter, W. D.; Coughlin, E. B.; Chacon, S. T.; Hajela, S.; Herzog, T. A.; Köhn, R.; Mitchell, J.; Piers, W. E.; Shapiro, P. J.; Bercaw, J. E. In *Ziegler Catalysts*; Fink, G., Mühlhaupt, R., Brintzinger, H.-H., Eds.; Springer-Verlag: Berlin, 1995; pp 317−331. (b) Edelmann, F. T. In *Metallocenes*; Togni, A., Haltermann, R. L., Eds.; Wiley-VCH: Weinheim, 1998; pp 55−110. (c) Chirik, P. J.; Bercaw, J. E. In *Metallocenes*; Togni, A., Haltermann, R. L., Eds., Wiley-VCH: Weinheim, 1998; pp 111−152.

(2) Maginn, R. E.; Manastyrskyj, S.; Dubeck, M. *J. Am. Chem. Soc.* **1963**, *85*, 672−676.

(3) Watson, P. L.; Parshall, G. W. *Acc. Chem. Res.* **1985**, *18*, 51−56.

(4) For recent reviews, see: Yasuda, H.; Tamai, H. *Prog. Polym. Sci.* **1993**, *18*, 1097−1139. (b) Yasuda, H. *Top. Organomet. Chem.* **1999**, 2, 255−283. (c) Yasuda, H.; Ihara, E. *Adv. Polym. Sci.* **1999**, *133*, 53−101.

(5) For recent reviews, see: (a) Edelmann, F. T. *Top. Curr. Chem.* **1996**, *179*, 247−276. (b) Anwander, R. In *Applied Homogeneous Catalysis with Organometallic Compounds*; Cornils, B., Herrmann, W. A., Eds.; VCH Publishers: Weinheim, 1996; pp 866−892. (c) Molander, G. A.: Dowdy, E. C. *Top. Organomet. Chem.* **1999**, *2*, 119−154.

(6) For examples, see: (a) Yasuda, H.; Yamamoto, H.; Yokota, K.; Miyake, S.; Nakamura, A. *J. Am. Chem. Soc.* **1992**, *114*, 4908−4910. (b) Giardello, M. A.; Yamamoto, Y.; Brard, L.; Marks, T. J. *J. Am. Chem. Soc.* **1995**, *117*, 3276−3279.

10.1021/ja992786a CCC: $19.00
Published on Web 03/18/2000

plexes of type **D** are the only reported single-site rare earth catalysts to be active in propene polymerization.[8] So far, salt metathesis starting from anhydrous lanthanide chlorides constitutes the only well-examined synthetic access to lanthanidocene derivatives of types **A**−**D**.[9,10] However, this route is encumbered by lengthy, tedious, often low-yield syntheses and ate complex formation, resulting in alkali metal- and donor solvent-contaminated products.[9,11]

Since metallocene-mediated stereoselective olefin transformation reactions are governed by ancillary ligand effects comprising steric and electronic factors as well as the induction of chirality, we thought it worthwhile to further investigate the class of C_2-symmetric lanthanidocene complexes. Strangely enough, few efforts have been made to extend the ligand spectrum to indenyl or fluorenyl congeners,[12] considering the benefits to research and industry which evolved from Brintzinger-type C_2-symmetric *ansa*-zirconocenes.[13] Recently, we communicated the synthesis of the first C_2-symmetric *ansa*-yttrocene complexes of type **E** according to an amine elimination reaction[14] which utilizes specialized silylamide complexes $Ln[N(SiHMe_2)_2]_3(THF)_x$ ($x = 1,2$) as synthetic precursors ("extended silylamide route").[15] The decreased steric bulk of the $[N(SiHMe_2)_2]$ ligand and THF dissociation are anticipated to render less shielded Ln−N bonds prone to extended proton-transfer reactions.[14,16−18] In addition, the thermally very stable "$Ln[N(SiHMe_2)_2]$" moiety enables ligand-exchange reactions at elevated temperatures and participates in strong diagostic $Ln\cdots(SiH)_2$ interactions. Also recently, in situ alkane elimination reactions, featuring $Ln(CH_2SiMe_3)_3(THF)_2$ as the reactive species, were successfully applied for the synthesis of linked amidocyclopentadienyl derivatives of type **F**.[19] However, the synthesis of the thermally labile tris(trimethylsilyl)methyl complexes is successful for the late lanthanide elements only and suffers from ate complexation.[20]

Here, we report on the feasibility of our extended silylamide route for the synthesis of C_2-symmetric *ansa*-lanthanidocene complexes of type **E** by considering a variety of representative ligands on the basis of steric and pK_a criteria.[21] A full account of the synthesis as well as spectroscopic and structural features of these complexes is presented. Companion contributions[22,23] will address (i) the strength and the features of the β-SiH diagostic interaction from a theoretical point of view and (ii) the kinetics and mechanism of complex racemizations as well as the implication of this diagostic interaction for the generation of high racemic yields.

Results and Discussion

Synthesis of *ansa*-Lanthanidocene Amides. The applicability of this extended silylamide route was initially probed for the routinely employed bis(2,3,4,5-tetramethyl-1-cyclopenta-2,4-dienyl)dimethylsilane ($[Me_2Si(CpH'')_2]$, **1**)[24] and subsequently applied to fused cyclopentadienyl ring systems including 2,2-bis(inden-1-yl)propane ($[Me_2C(IndH)_2]$, **2**), bis(2-methylinden-1-yl)dimethylsilane ($[Me_2Si(2\text{-}Me\text{-}IndH)_2]$, **3**), bis(2-methyl-4-phenylinden-1-yl)dimethylsilane ($[Me_2Si(2\text{-}Me\text{-}4\text{-}Ph\text{-}IndH)_2]$, **4**), bis(2-methyl-4,5-benzoinden-1-yl)dimethylsilane ($[Me_2Si(2\text{-}Me\text{-}Benz\text{-}IndH)_2]$, **5**), and bis(fluoren-9-yl)dimethylsilane ($[Me_2Si(FluoH)_2]$, **6**).[25,26] According to Scheme 1, reaction with the bis(dimethylsilyl)amide precursors **7a**−**c**[16] gave the corresponding *ansa*-lanthanidocene amide complexes.

^{1}H NMR spectroscopy and GC−MS analysis revealed that complete conversion is achieved only at elevated temperatures.

(7) Arredondo, V. M.; Tian, S.; McDonald, F. E.; Marks, T. J. *J. Am. Chem. Soc.* **1999**, *121*, 3633−3639 and references therein.

(8) Mitchell, J. P.; Hajela, S.; Brookhart, S. K.; Hardcastle, K. I.; Henling, L. M.; Bercaw, J. E. *J. Am. Chem. Soc.* **1996**, *118*, 1045−1053.

(9) For recent organolanthanide reviews, see: (a) Schumann, H.; Meese-Marktscheffel, J. A.; Esser, L. *Chem. Rev.* **1995**, *95*, 865−986. (b) Edelmann, F. T. In *Comprehensive Organometallic Chemistry II*; Abel, E. W., Stone, F. G. A., Wilkinson, G., Eds.; Pergamon: Oxford, 1995; Vol. 4, pp 11−212.

(10) Alternative methods of preparation have only rarely been undertaken: (a) Fischer, E. O.; Fischer, H. *Angew. Chem.* **1964**, *76*, 52. (b) Hammel, H.; Weidlein, J. *J. Organomet. Chem.* **1990**, *388*, 75−87. (c) Watson, P. L.; Whitney, J. F.; Harlow, R. L. *Inorg. Chem.* **1981**, *20*, 3271−3278. (d) Stults, S. D.; Andersen, R. A.; Zalkin, A. *Organometallics* **1990**, *9*, 115−122. (e) Mu, Y.; Piers, P. E.; MacDonald, M.-A.; Zaworotko, M. J. *Can. J. Chem.* **1995**, *73*, 2233−2238. (f) For further non-salt metathesis routes to organolanthanide complexes, see: Schaverien, C. J. *Adv. Organomet. Chem.* **1994**, *36*, 283−362.

(11) Alkali metal ligand ate complexation was reported to markedly affect the stereoselectivity of acrylate polymerization: Yasuda, H.; Ihara, E. *Macromol. Chem. Phys.* **1995**, *196*, 2417−2441.

(12) (a) Deacon, G. B.; Newnham, R. H. *Aust. J. Chem.* **1985**, *38*, 1757−1765. (b) Evans, W. J.; Gummersheimer, T. S.; Boyle, T. J.; Ziller, J. W. *Organometallics* **1994**, *13*, 1281−1284. (c) Wang, S.; Yu, Y.; Ye, Z.; Qian, C.; Huang, X. *J. Organomet. Chem.* **1994**, *464*, 55−58. (d) Qian, C.; Zou, G.; Sun, J. *J. Organomet. Chem.* **1998**, *566*, 21−28. (e) Kretschmer, W. P.; Troyanov, S. I.; Meetsma, A.; Hessen, B.; Teuben, J. H. *Organometallics* **1998**, *17*, 284−286.

(13) For a recent review, see: Brintzinger, H.-H.; Fischer, D.; Mülhaupt, R.; Rieger, B.; Waymouth, R. M. *Angew. Chem.* **1995**, *107*, 1255−1283; *Angew. Chem., Int. Ed. Engl.* **1995**, *34*, 1143−1170.

(14) Herrmann, W. A.; Eppinger, J.; Runte, O.; Spiegler, M.; Anwander, R. *Organometallics* **1997**, *16*, 1813−1814.

(15) Anwander, R.; Runte, O.; Eppinger, J.; Gerstberger, G.; Spiegler, M.; Herdtweck, E. *J. Chem. Soc., Dalton Trans.* **1998**, 847−858.

(16) Anwander, R. *Top. Curr. Chem.* **1996**, *179*, 33−112 and literature cited therein. For examples utilizing this specialized amide precursor, see: (a) Runte, O.; Priermeier, T.; Anwander, R. *J. Chem. Soc., Chem. Commun.* **1996**, 1385−1386. (b) Görlitzer, H. W.; Spiegler, M.; Anwander, R. *Eur. J. Inorg. Chem.* **1998**, 1009−1014.

(17) In contrast, efforts to synthesize lanthanidocene complexes from $Ln[N(SiMe_3)_2]_3$ precursor compounds were successful in moderate yields only for derivatives featuring nonlinked cyclopentadienyl ligands and the larger lanthanide(III) cations (Ln = La, Ce, Sm): Booij, M.; Kiers, N. H.; Heeres, H. J.; Teuben, J. H. *J. Organomet. Chem.* **1989**, *364*, 79−86.

(18) The amine elimination reaction as a route to zirconocene complexes is meanwhile established: (a) Chandra, G.; Lappert, M. F. *J. Chem. Soc. A* **1968**, 1940−1945. (b) Hughes, A. K.; Meetsma, A.; Teuben, J. H. *Organometallics* **1993**, *12*, 1936−1945. (c) Herrmann, W. A.; Morawietz, M. J. A.; Priermeier, T. *Angew. Chem.* **1994**, *106*, 2025−2028; *Angew. Chem., Int. Ed. Engl.* **1994**, *33*, 1946−1949. (d) Diamond, G. M.; Jordan, R. F.; Petersen, J. L. *Organometallics* **1997**, *16*, 3044−3055 and references therein.

(19) (a) Mu, Y.; Piers, W. E.; MacQuarnie, D. C.; Zaworotko, M. J.; Young, U. G., Jr. *Organometallics* **1996**, *15*, 2720−2726. (b) Hultzsch, K. C.; Spaniol, T. P.; Okuda, J. *Angew. Chem.* **1999**, *111*, 163−166; *Angew. Chem., Int. Ed. Engl.* **1999**, *38*, 227−230.

(20) (a) Lappert, M. F.; Pearce, R. *J. Chem. Soc., Chem. Commun.* **1973**, 126. (b) Schumann, H.; Müller, J. *J. Organomet. Chem.* **1978**, *146*, C5−C7.

(21) Parts of this work were already communicated: (a) Anwander, R.; Eppinger, J., Spiegler, M. 214th National Meeting of the American Chemical Society, September 7−11, 1997, Las Vegas, NV. (b) Eppinger, J.; Spiegler, M.; Anwander, R. X. Workshop on Rare Earth Elements, December 3−5, 1997, Berlin, Germany.

(22) Hieringer, W.; Eppinger, J.; Anwander, R.; Herrmann, W. A. *J. Am. Chem. Soc.*, in press.

(23) (a) Eppinger, J. Ph.D. Thesis, Technische Universität München, 1999. (b) Eppinger, J.; Spiegler, M.; Herrmann, W. A.; Anwander, R., unpublished results.

(24) Jutzi, P. Dickbreder, R. *Chem. Ber.* **1986**, *119*, 1750−1754.

(25) For ligand synthesis, see the following. (a) $Me_2C(IndH)_2$: Nifant'ev, I. E.; Ivchenko, P. V.; Kuz'mina, G.; Luzikov, Y. N.; Sitnikov, A. A.; Sizan, O. E. *Synthesis* **1997**, 469−474. (b) $Me_2Si(2\text{-}Me\text{-}IndH)_2$: Spaleck, W.; Antberger, M.; Rohrmann, J.; Winter, A.; Bachmann, B.; Kiprof, P.; Behm, J.; Herrmann, W. A. *Angew. Chem.* **1992**, *104*, 1373−1376; *Angew. Chem., Int. Ed. Engl.* **1992**, *32*, 1345−1347. (c) $Me_2Si(2\text{-}Me\text{-}4\text{-}Ph\text{-}IndH)_2$: Spaleck, W.; Küber, F.; Winter, A.; M.; Rohrmann, J.; Bachmann, B.; Antberger, M.; Dolle, V.; Paulus, E. P. *Organometallics* **1994**, *13*, 954−963. (d) $Me_2Si(2\text{-}Me\text{-}Benz\text{-}IndH)_2$: Stehling, U.; Diebold, J.; Kirsten, R.; Roll, W.; Brintzinger, H.-H.; Jüngling, S.; Mühlhaupt, R.; Langhauser, F. *Organometallics* **1994**, *13*, 963−970. (e) For a comparable survey of structural parameters in zirconocene chlorides, see: Resconi, L.; Piemontesi, F.; Camurato, I.; Sumeijer, O.; Nifant'ev, I. E.; Ivchenko, P. V.; Kuz'mina, L. G. *J. Am Chem. Soc.* **1998**, *120*, 2308−2321.

(26) Chen, Y.-X.; Rausch, M. D.; Chien, J. C. W. *J. Organomet. Chem.* **1995**, *497*, 1−9.

Scheme 1. Synthesis of C_2-Symmetric *ansa*-Lanthanidocene Amide Complexes According to the Extended Silylamide Route

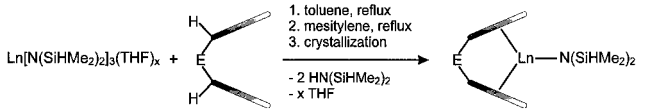

	E	ligand precursor	Ln (yield)	
	$(CH_3)_2Si$	$Me_2Si(Cp''H)_2$ (**1**)	Y (82%) La (96%)	**11b** **11c**
	$(CH_3)_2C$	$Me_2C(IndH)_2$ (**2**)	*rac*-Y (14%)	*rac*-**12b**
	$(CH_3)_2Si$	$Me_2Si(2\text{-Me-IndH})_2$ (**3**)	*rac*-Sc (20%) *rac*-Y (52%) *rac*-La (49%) *rac*-Nd (44%) *rac*-Lu (32%)	*rac*-**13a** *rac*-**13b** *rac*-**13c** *rac*-**13d** *rac*-**13e**
	$(CH_3)_2Si$	$Me_2Si(2\text{-Me-4-Ph-IndH})_2$ (**4**)	Y (11%)[a] *rac*-La (13%)	**14b** *rac*-**14c**
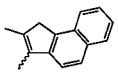	$(CH_3)_2Si$	$Me_2Si(2\text{-Me-4,5-Benz-IndH})_2$ (**5**)	*rac*-Y (72%) *rac*-La (47%) *rac*-Lu (54%)	*rac*-**15b** *rac*-**15c** *rac*-**15e**
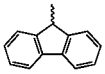	$(CH_3)_2Si$	$Me_2Si(FluoH)_2$ (**6**)	Y (7%)[b]	**16b**

[a] Monocoordination of the *ansa*-ligand detected only. [b] Complex detected by NMR spectroscopy only.

Recrystallization of the crude reaction products from *n*-hexane or toluene solutions afforded the pure compounds. The overall yield of the homologous bis(dimethylsilyl)amide complexes $[SiMe_2(C_5Me_4)_2]Ln[N(SiHMe_2)_2]$ (**11b**,**c**) is almost double that of the corresponding bis(trimethylsilyl)amide derivatives $[SiMe_2(C_5Me_4)_2]Ln[N(SiMe_3)_2]$ obtained by conventional salt metathesis.[27]

Crystallization of the *ansa*-bis(indenyl) complexes afforded the pure *rac*-form in moderate to good yields. The *meso*-derivatives were obtained as THF adducts which could not be isolated in pure form. NMR spectra of the *meso*-isomers usually display broad signals at room temperature.[22] The yields of the *rac*-isomers could be increased by prolonged thermal treatment via consecutive refluxing in toluene and mesitylene (two-step synthesis). This enrichment of the *rac*-form can be explained in terms of donor (THF) evaporation during boiling and a *rac*/*meso* equilibrium shift due to donor displacement.[22]

Use of the $SiMe_2$-linked indene **3** carrying a methyl group in the 2-position resulted in the isolation of the first Brintzinger-type *ansa*-lanthanidocene complexes **13**.[16] The development of the two-step synthesis allowed the synthesis of *ansa*-indenyl complexes covering the entire range of rare earth cation radii. However, formation of derivatives of the smaller Sc(III) and Lu(III) was hampered by long reaction times and moderate racemic yields. The highest racemic yields were achieved for medium-sized yttrium in complex **13b**. Attempts to synthesize the corresponding bis(trimethylsilyl)amide complex from **3** and $Y[N(SiMe_3)_2]_3$ failed due to decomposition reactions during prolonged heating.[18,28] This finding emphasizes the necessity for synthetic precursors carrying sterically more flexible, readily exchangeable amide ligands.

The reactivity of indene **4** featuring phenyl substitution in the 4-position was markedly decreased. Only for the larger La(III) cation could an *ansa*-complex be isolated (*rac*-**14c**). The putative yttrium complex could not be obtained. Instead, monocoordination of the ancillary ligand was observed to yield $[Me_2Si(2\text{-Me-4-Ph-Ind})_2H]Y[N(SiHMe_2)_2]_2$ (**14b**), which can be seen as a reaction intermediate of the *ansa*-complex formation according to Scheme 3. The yield of the pure yttrium complex *rac*-**12b** derived from the propylidene-bridged indenyl ligand was also low. This can be attributed to a more opened coordination sphere at the metal center, arising from the absence of a methyl group in the 2-position and a short propylidene *ansa*-bridge. The increased bite angle of the ligand enhances the electron deficiency of the metal center, which disfavors donor (THF) dissociation, the latter being a prerequisite of high racemic yields. The attempted synthesis of the corresponding lanthanum complex **12c** is in accord with this finding: the larger lanthanum center discourages the *ansa*-coordination mode, probably forming an oligomeric product which is barely soluble in tetrahydrofuran.

Scheme 2. Utilization of a Linked 4,5-Substituted Benzoindene System **5** for the Synthesis of the *ansa*-Yttrocene Amide Complex **15b** According to the Extended Silylamide Route (**5** = $(2\text{-Me-Benz-IndH})_2SiMe_2$; R = $SiHMe_2$)[a]

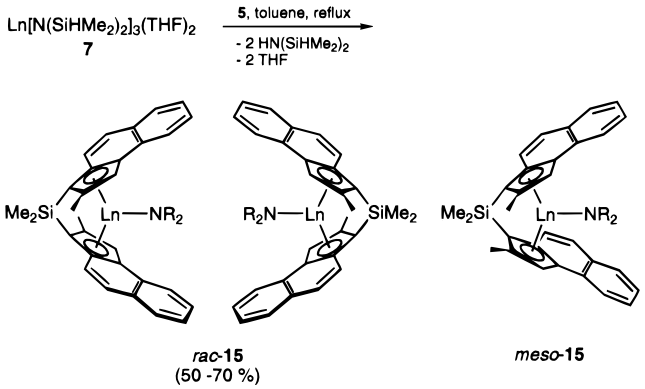

[a] The *meso*-isomer was detected as mono-THF adduct by NMR spectroscopy.

In contrast, the 4,5-substituted benzoindene **5** exhibits substantially higher reactivity, and the resulting complexes **15** reveal amazingly high racemic yields (Scheme 2). The implications of the 4,5-benzo substitution vs the 4-phenyl substitution for the synthetic outcome will be discussed below. The lower yield of the lanthanum derivative **15c** compared to the homologous yttrium compound **15b** probably reflects the tendency for Si−C bond-breaking during the synthesis of these complexes at elevated temperatures.[22] Bis(fluorene) **6** gave roughly a 7% yield of complex **16b** as detected by ^1H NMR.

Elemental analyses of complexes **11**, **12**, **13**, and **15** are consistent with complete THF displacement at the metal center. The enhanced thermal stability of the novel *ansa*-lanthanidocene complexes is also revealed by their CI mass spectra. In addition to the intense peaks of the parent molecular ions, fragmentation occurred mainly due to methyl- and bis(dimethylsilyl)amide separation. A dinuclear species was detected for the isopropylidene-bridged derivative **12b**, pointing out redistribution reactions of the ancillary ligand.[29] All of the isolated bis(cyclopentadienyl) and *rac*-bis(indenyl) metallocene amide complexes

(27) Giardello, M. A.; Conticelli, V. P.; Brard, L.; Sabat, M.; Rheingold, A. L.; Stern, C. L.; Marks, T. J. *J. Am. Chem. Soc.* **1994**, *116*, 10212−10240.

(28) Addition of tetramethyldisilazane to the $Y[N(SiMe_3)_2]_3$ reaction will also initiate the "diene"/silylamine ligand exchange; however, this procedure is prone to side products: Eppinger, J.; Anwander, R., unpublished results.

Table 1. Selected IR and NMR Spectroscopic Data for Bis(dimethylsilyl)amide Complexes

compound	IR[a] $\nu_{(SiH)}$ (cm^{-1})	^{1}H NMR[b] $\delta_{(SiH)}$ (ppm)	^{29}Si NMR[b] $\delta_{(Si)}$ (ppm) ($^1J_{Si,H}$)
$[Me_2Si(Cp'')_2]YN(SiHMe_2)_2$ (**11b**)	1789	4.00 (dsp)	−19.9 (147)
$[Me_2Si(Cp'')_2]LaN(SiHMe_2)_2$ (**11c**)	1845	4.18 (m)	−17.3 (150)
rac-$[Me_2C(Ind)_2]YN(SiHMe_2)_2$ (*rac*-**12b**)	1821	3.56 (dsp)[c]	− (152)
rac-$[Me_2Si(2\text{-}Me\text{-}Ind)_2]ScN(SiHMe_2)_2$ (*rac*-**13a**)	2012/1793	2.96 (m)	− (155)
rac-$[Me_2Si(2\text{-}Me\text{-}Ind)_2]YN(SiHMe_2)_2$ (*rac*-**13b**)	1804	2.97 (dsp)[c]	− (142)
rac-$[Me_2Si(2\text{-}Me\text{-}Ind)_2]LaN(SiHMe_2)_2$ (*rac*-**13c**)	1838	3.74 (m)	− (145)
rac-$[Me_2Si(2\text{-}Me\text{-}Ind)_2]NdN(SiHMe_2)_2$ (*rac*-**13d**)	1824	—[d]	—[d]
rac-$[Me_2Si(2\text{-}Me\text{-}Ind)_2]LuN(SiHMe_2)_2$ (*rac*-**13e**)	1759	3.29 (sp)[c]	− (146)
$[Me_2Si(2\text{-}Me\text{-}4\text{-}Ph\text{-}Ind)_2H]Y[N(SiHMe_2)_2]_2$ (**14b**)	2069/1830	4.31 (dsp)	− (148)
rac-$[Me_2Si(2\text{-}Me\text{-}4\text{-}Ph\text{-}Ind)_2]LaN(SiHMe_2)_2$ (*rac*-**14c**)	1832	3.87 (m)	− (141)
rac-$[Me_2Si(2\text{-}Me\text{-}Benz\text{-}Ind)_2]YN(SiHMe_2)_2$ (*rac*-**15b**)	1811	2.65 (dsp)[c]	−26.6 (133)
rac-$[Me_2Si(2\text{-}Me\text{-}Benz\text{-}Ind)_2]LaN(SiHMe_2)_2$ (*rac*-**15c**)	1838	3.30 (m)	− (140)
rac-$[Me_2Si(2\text{-}Me\text{-}Benz\text{-}Ind)_2]LuN(SiHMe_2)_2$ (*rac*-**15e**)	1773	2.98 (sp)[c]	− (142)
$[Me_2Si(Fluo)_2]YN(SiHMe_2)_2$ (**16b**)	—[e]	3.21 (sp)	—[f]
$Ln[N(SiHMe_2)_2]_3(THF)_x$ (**7**, $x = 1, 2$) (ref 16)	2051−2072, 1931−1970 (sh)	4.94−5.02 (sp)	−19.3 to −26.0 (162−171)
$\{ZrCl[N(SiHMe_2)_2]_2(\mu\text{-}Cl)\}_2$ (ref 30)	2136, 2093, 1948	5.06 (sp)	−

[a] IR spectra were recorded as Nujol mulls. [b] NMR spectra were recorded at 25 °C as C_6D_6 solutions. [c] The coupling pattern is of higher order and rather describes the signal shape. [d] The SiH signal could not be detected due to the paramagnetic neodymium center. [e] As the isolation of **16b** failed, no IR spectrum could be recorded. [f] The detection of the silicon sidebands was not sufficient for an accurate determination of the $^1J_{Si,H}$ coupling constant.

display good solubility in warm hydrocarbons, which facilitated their spectroscopic characterization.

Spectroscopic Characterization. The IR spectra of all of the isolated rare earth metallocene bis(dimethylsilyl)amide complexes show a distinct shift (>200 cm^{-1}) of the Si−H stretching frequency to lower energy in comparison to the synthetic precursors **7a**−**c** (ca. 2060 cm^{-1}) (see Table 1).[16] This behavior is particularly pronounced for the smaller cations, indicating the effect of enhanced Lewis acidity. The lutetium complex *rac*-**13e** displays a shift as large as 312 cm^{-1}. In general, such a distinct Si−H bond-weakening is assigned to agostic interactions.[30−32] In fact, these Si−H stretching frequencies are significantly lower than those observed for β-SiH interactions in early transition metal complexes.[32] The bonding mode seems to be even comparable to that in Mo-η^2(Si−H) complexes (1750−1730 cm^{-1}).[33]

The IR spectrum of the scandium derivative *rac*-**13a** shows two well-separated Si−H stretching vibrations, while the spectra of the lanthanum, yttrium, and lutetium complexes display a less intense and broadened Si−H band, excluding a more detailed interpretation. Interestingly, the scandium complex also shows a band at 1072 cm^{-1} attributable to a $\nu_{as}(NSi_2)$ stretching vibration which reinforces evidence for different coordination modes of the $Ln-N(SiHMe_2)_2$ moiety.

NMR spectroscopic examinations of the diamagnetic complexes **11b**,**c**, *rac*-**12b**, *rac*-**13a**−**c**,**e**, **14b**, *rac*-**14c**, *rac*-**15b**,**c**, and **16b** were performed to clarify the significant perturbation of the SiH environment. The findings are discussed for the yttrium complexes in more detail. The ^{1}H NMR spectrum of *rac*-**13b** is representatively shown in Figure 2.

A strong dependency of the SiH signal on the nature of the metal center and the ligands was observed. In accordance with the IR spectra, the smaller metal cations induce a larger upfield shift of the SiH signal, correlating with an enhanced agostic interaction of the more Lewis acidic metal center. The ^{1}H NMR spectrum of *rac*-**15b** shows a SiH resonance at 2.65 ppm which is 2.33 ppm upfield compared to the signal of **7b** (Table 1). Such drastic upfield shifts were also found in related zirconocene complexes.[32] In addition, the dramatic Si−H upfield shifts seem to be associated with the presence of extended aromatic ring systems, increasing in the order **1** < **2**, **3**, **4** < **5** < **6**.[34,35]

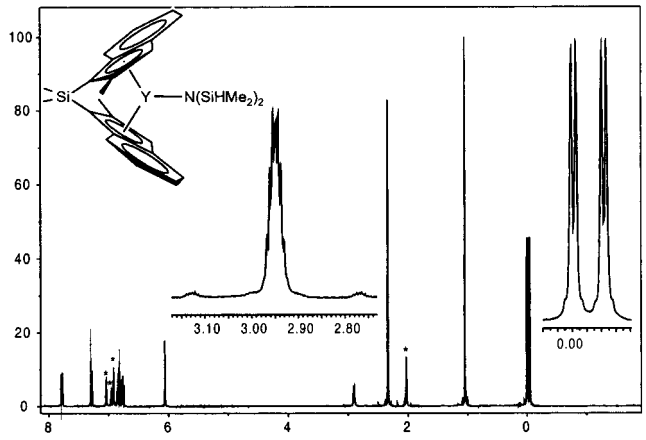

Figure 2. ^{1}H NMR spectrum (400 MHz) of $[Me_2Si(2\text{-}Me\text{-}Ind)_2]Y[N(SiHMe_2)_2]$ (**13b**) as a solution in toluene-d_8. The solvent signals are indicated by an asterisk.

Examination of the SiH coupling pattern indicates the presence of a $J_{Ln,H}$ coupling in all of the *ansa*-metallocene amide complexes. Whereas the complexes of the metals with $I > {}^1/_2$ (Sc, La, Lu) produce poorly resolved multiplets, the SiH resonances of the yttrocene amide complexes resemble a nonet, which is derived from a doublet of septets, as peak intensities suggest. The doublet splitting in the range of 2.9 (**11b**)−5.0 Hz (*rac*-**15b**) which occurs in addition to the $^3J_{H,H}$ coupling (about 2.5 Hz) can be assigned to a H···Y···H coupling.[36] Relatively small ^{1}H−^{29}Si coupling constants document a significant lengthening of the SiH bond (Table 1),[37] the value of 133 Hz for *rac*-**15b** suggesting a considerable activation of

(29) (a) Höck, N.; Oroschin, W.; Paolucci, G.; Fischer, R. D. *Angew. Chem.* **1986**, *98*, 748−749; *Angew. Chem., Int. Ed. Engl.* **1986**, *25*, 738−739. (b) Stern, D.; Sabat, M.; Marks, T. J. *J. Am. Chem. Soc.* **1990**, *112*, 9558−9575.

(30) Herrmann, W. A.; Huber, N. W.; Behm, J. *Chem. Ber.* **1992**, *125*, 1405−1407.

(31) Rees, W. S.; Just, O.; Schumann, H.; Weimann, R. *Angew. Chem.* **1996**, *108*, 481−483; *Angew. Chem., Int. Ed. Engl.* **1996**, *35*, 419−422.

(32) Procopio, L. J.; Carrott, J. J.; Berry, D. H. *J. Am. Chem. Soc.* **1994**, *116*, 177−185.

(33) Lou, X. J.; Kubas, G. J.; Burns, C. J.; Bryan, J. C.; Unkefer, C. J. *J. Am. Chem. Soc.* **1995**, *117*, 1159−1160.

(34) For the interpretation of analogous upfield shifts due to aromatic ring currents, see: (a) Haigh, C. W.; Mallion, R. B. *Prog. Nucl. Magn. Reson. Spectrosc.* **1980**, *13*, 303−344. (b) Haigh, C. W.; Mallion, R. B. *Org. Magn. Reson.* **1972**, *4*, 203−228.

(35) Calculations on the basis of the model of Haigh and Mallion[34] point out that the ring current only partly contributes to the high upfield shift of the SiH proton.

the Si−H bond by metal coordination.[33,38,39] The recorded ^{29}Si resonances range from −26.6 (*rac*-**11b**) to −17.3 (*rac*-**15b**) and from −32.5 (*rac*-**11b**) to −15.9 ppm (*rac*-**15b**) for N(*Si*HMe$_2$)$_2$ and the *Si*Me$_2$-*ansa*-bridge, respectively. The proton-decoupled ^{29}Si NMR spectrum of *rac*-**15b** displays two doublets due to ^{29}Si−^{89}Y coupling of both the dimethylsilylamide moiety (12.2 Hz) and the dimethylsilyl bridge (1.2 Hz).[40] Perhaps the most striking feature of the new *ansa*-metallocene amide complexes is their rigidity in solution, as evidenced by the persistence of the H···Y···H coupling. The ^{1}H NMR spectra of complexes **13a**,**b** and **15b** in toluene-d_8 reveal the absence of any significant signal shift or change of coupling pattern in the temperature range from −90 to 130 °C. The ^{1}H and ^{13}C resonances of the methylsilyl(amido) group of the racemic compounds appear as two doublets and a doubled singlet, respectively, as expected for two methyl groups with different chemical environments. In contrast, the C_{2v}-symmetric complexes **11b** and **11c** display only one doublet and a singlet, respectively. However, the latter complexes show the same SiH coupling pattern as the C_2-symmetric derivatives, indicating that this coupling pattern results from Ln−H coupling and not from the diastereotopy of the two methyl groups.

The presence of a Y−H coupling was unequivocally proven by ^{89}Y NMR spectroscopy. The ^{89}Y NMR spectrum of *rac*-**15b** shows a triplet with a ^{89}Y−^{1}H coupling constant of 4.7 Hz (Figure 3b). This relatively small coupling constant[41] is in good agreement with the value derived from the ^{1}H NMR spectrum ($J_{Y,H}$ = 5.0 Hz). The visible ^{29}Si satellites display a coupling constant of 19.5 Hz.[40] The shielding ring current of the aromatic indenyl ligands results in a dramatic upfield shift of the ^{89}Y signal to −96.7 ppm compared to that of the amide precursor **7b** (δ = 444 ppm).[16,42] The distinct temperature dependency of this chemical shift was demonstrated by measurements at ca. 25 °C (δ = −96.7 ppm) and constant 30 °C (δ = −93.5 ppm).

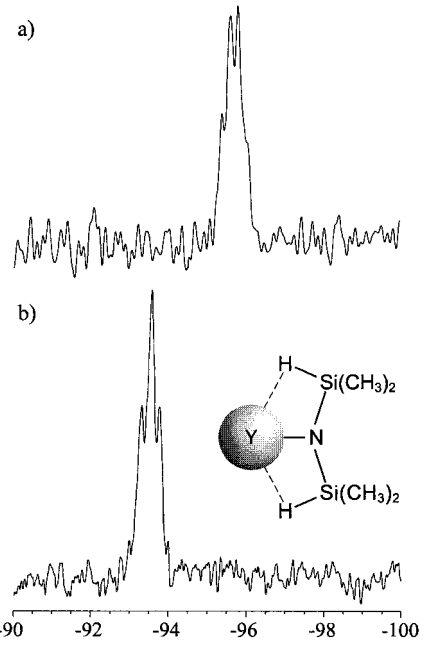

Figure 3. ^{89}Y NMR spectra of *rac*-**15b** without (ca. 25 °C; a) and with (30.0 ± 0.1 °C; b) temperature control.

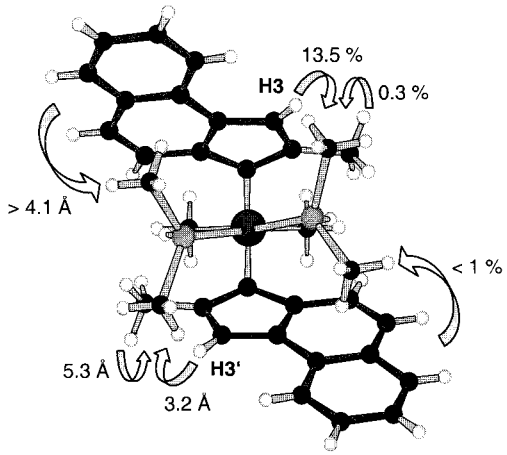

Figure 4. NOE enhancements and solid-state structure bonding distances of the two diastereotopic methyl groups of the amide moiety of *rac*-**15b**.

Without temperature regulation, the signal appears as a noninterpretable pseudoquartet (Figure 3a).[43]

The β-SiH agostic rigidity of the amide fragment could be further corroborated by ^{1}H NMR−NOE spectroscopy of *rac*-**15b**. Due to the fixed arrangement, the two diastereotopic methyl(silylamide) groups display only one intense NOE signal between the less upfield-shifted methyl resonance and the signal of the hydrogen atom H3 of the benzoindenyl moiety (13.5% enhancement). All of the other enhancements resulting from proton coupling with the amide ligand fragment are below 1% (Figure 4). These findings are in accordance with the observed distances in the solid-state structure which reveal a relatively close contact of ca. 3.2 Å between the averaged methyl hydrogen atoms of the amide ligand and the H3 hydrogen atom. This

(36) The size of the coupling constant is attributable to a $^3J_{Y,SiH}$ coupling rather than a $^1J_{Y,H}$ one. The higher order coupling pattern of the SiH proton in the *rac*-form can be assigned to coupling with two diastereotopic methyl groups or additional through-space $J_{H,H}$ coupling via Y.

(37) Lukevics, E.; Pudowa, O.; Sturkovich, R. *Molecular Structure of Organosilicon Compounds*; Ellis-Horwood: Chichester, U.K., 1989. Silicon hydrides generally display $^1J_{Si,H}$ values in the range 160−200 cm^{-1}.

(38) $^1J_{Si,H}$ values for M-(η^2-SiH). (a) 136 Hz for M = Cr: Driess, M.; Reigys, M.; Pritzkow, H. *Angew. Chem.* **1992**, *104*, 1514−1516; *Angew. Chem., Int. Ed. Engl.* **1992**, *31*, 1510−1512. (b) 92 Hz for M = Ti: Ohff, A.; Kosse, P.; Baumann, W.; Tillack, A.; Kempe, R.; Görls, H.; Burlakov, V. V.; Rosenthal, U. *J. Am. Chem. Soc.* **1995**, *117*, 10399−10400. (c) 20−70 Hz for M = Mo: Luo, X.-L.; Kubas, G. J.; Bryan, J. C.; Burns. J. C.; Unkefer, C. J. *J. Am. Chem. Soc.* **1994**, *116*, 10312−10313. (d) Crabtree, R. H.; Pritzkow, H. *Angew. Chem.* **1993**, *105*, 828−845; *Angew. Chem., Int. Ed. Engl.* **1993**, *32*, 789−805. (e) Crabtree, R. H.; Hamilton, D. G. *Adv. Organomet. Chem.* **1988**, *28*, 299−358. (f) Schubert, H. *Adv. Organomet. Chem.* **1990**, *30*, 151−187.

(39) σ-Bond metathesis reactions involving Ln−C/Si−H transpositions were reported to occur in hydrosilylation reactions: (a) Sakura, T.; Lautenschlager, H.-J.; Tanaka, M. *J. Chem. Soc., Chem. Commun.* **1991**, 40−41. (b) Molander, G. A.; Julius, M. *J. Org. Chem.* **1992**, *57*, 6347−6351. (c) Onozawa, S.; Sakakura, T.; Tanaka, M. *Tetrahedron Lett.* **1994**, *35*, 8177−8180. (d) Ziegler, T.; Folga, E. *J. Organomet. Chem.* **1994**, *478*, 57−65. (e) Molander, G. A.; Nichols, P. J. *J. Am. Chem. Soc.* **1995**, *117*, 4415−4416. (f) Radu, N. S.; Tilley, T. D. *J. Am. Chem. Soc.* **1995**, *117*, 5863−5864. (g) Fu, P.-F.; Brard, L.; Li, Y.; Marks, T. J. *J. Am. Chem. Soc.* **1995**, *117*, 7157−7168. (h) Voskoboynikov, A. Z.; Parshina, I. N.; Shestakova, A. K.; Butin, K. P.; Beletskaya, I. P.; Kuz'mina, L. G.; Howard, J. A. K. *Organometallics* **1997**, *16*, 4041−4055.

(40) A $^2J_{Si,Y}$ coupling constant of 7.7 Hz was reported for a siloxide complex, Y$_2$(OSiPh$_3$)$_6$: Coan, P. S.; Hubert-Pfalzgraf, L. G.; Caulton, K. G. *Inorg. Chem.* **1992**, *31*, 1262−1267.

(41) $^1J_{Y,H}$ coupling constants are in the range of 15−30 Hz: Rheder, D. In *Transition Metal Nuclear Magnetic Resonance*; Pregosin, P. S., Ed.; Elsevier: Amsterdam, 1991; pp 4−51. $^2J_{Y,H}$ = 3.6 Hz for the Y(μ-CH$_3$)Y moiety in [(CH$_3$C$_5$H$_4$)$_2$Y(μ-CH$_3$)]$_2$: Evans, W. J.; Meadows, J. H.; Wayda, A. L.; Hunter, W. E.; Attwood, J. L. *J. Am. Chem. Soc.* **1982**, *104*, 2008−2014.

(42) For a systematic investigation of ^{89}Y chemical shifts in metal−organic compounds, see: (a) Evans, W. J.; Meadows, J. H.; Kostka, A. G.; Closs, G. L. *Organometallics* **1985**, *4*, 324−326. (b) Schaverien, C. J. *Organometallics* **1994**, *13*, 69−82.

(43) Similar effects have been reported for ^{103}Rh NMR: Mann, B. E. In *Transition Metal Nuclear Magnetic Resonance*; Pregosin, P. S., Ed.; Elsevier: Amsterdam, 1991; pp 177−215.

Table 2. Selected Structural Parameters for Lanthanidocene Complexes

	11c (Ln = La)	*rac*-**13b**[c] (Ln = Y)	*rac*-**13e**[c] (Ln = Lu)	*rac*-**15b** (Ln = Y)	*rac*-**15e** (Ln = Lu)
			Bond Distances (Å)		
av. Ln1−C_{Cp}	2.799	2.663	2.614	2.666	2.627
min. Ln1−C_{Cp}	2.738(2)	2.627(3)	2.574(3)	2.609(3)	2.577(6)
max. Ln1−C_{Cp}	2.867(3)	2.697(3)	2.651(3)	2.719(4)	2.670(6)
Ln1−C_g1[a]	2.523(1)	2.371(2)	2.315(2)	2.378(2)	2.328(2)
Ln1-C_g2[a]	2.526(1)	2.371(2)	2.315(2)	2.372(2)	2.327(2)
Ln1-N1	2.449(3)	2.237(4)	2.159(4)	2.274(3)	2.173(5)
Ln1−Si1	3.246(1)	3.082(1)	3.116(1)	3.028(1)	3.277(2)
Ln1−Si2	3.244(1)	3.082(1)	3.116(1)	3.034(1)	3.041(2)
Ln1−Si3	3.494(1)	3.387(2)	3.347(1)	3.416(1)	3.384(2)
Ln1−H1[b]	2.70(3)	2.54(2)	2.63(2)	2.37(3)	3.05(2)
Ln1−H2[b]	2.66(4)	2.54(2)	2.63(2)	2.38(3)	2.66(2)
N1−Si1	1.661(3)	1.666(1)	1.676(2)	1.660(3)	1.656(6)
N1−Si2	1.663(3)	1.666(1)	1.676(2)	1.661(3)	1.682(6)
Si1−H1[b]	1.39(3)	1.45(2)	1.42(5)	1.45(3)	1.45(2)
Si2−H2[b]	1.38(4)	1.45(2)	1.42(5)	1.47(3)	1.45(2)
			Bond Angles (deg)		
C_g1−Ln1−C_g2[a]	118.53(2)	123.14(2)	125.3(2)	122.75(1)	124.58(2)
Si1−N1−Si2	154.9(2)	153.3(2)	144.0(2)	160.1(2)	139.3(4)
Ln1-N1−Si1	102.6(1)	103.4(1)	108.0(1)	99.5(2)	117.1(3)
Ln1-N1−Si2	102.5(1)	103.4(1)	108.0(1)	99.7(1)	103.4(3)
N1−Si1−H1	103(1)	100(1)	98(2)	98(1)	103.7
N1−Si2−H2	101(2)	100(1)	98(2)	98(1)	104.6
H1-Ln1-H2	109(1)	119.1(8)	115.6(14)	121.4(10)	113.4
			Dihedral Angles (deg)		
Ln1-N1−Si1−H1	−1(1)	3(1)	4.3(2)	6(1)	−11.5
Ln1-N1−Si2−H2	4(2)	−3(1)	−4.3(2)	3(1)	−7.8

[a] C_g = ring centroid. [b] Ln−H and Si−H distances have to be discussed carefully due to the location of the hydrogen atoms close to two heavy atoms. [c] As the metallocenes *rac*-**13b** und *rac*-**13e** crystallize in a *C*2/*c*-symmetric unit cell, the atoms were labeled differently: $C_g2 = C_g1a$; Si1 = Si2; Si2 = Si2a; Si3 = Si1; H1 = H2; H2 = H2a.

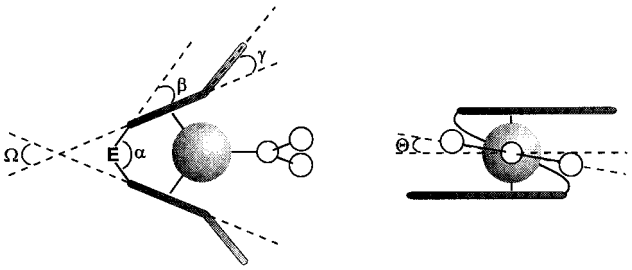

Figure 5. Definition of twisted geometry angles summarized in Table 3.

rigidity of the silylamide moiety explains the strong dependency of the Si−H upfield shift on the type of *ansa*-ligand as described above: the SiH group located below the shielding ring current[34,35] of the aromatic ligand is sensitive toward both a decreasing cationic radius and extension of the fused aromatic rings into the environment of the amide fragment.

Molecular Structures of the *ansa*-Lanthanidocene Amides 11c, *rac*-13b, *rac*-13e, *rac*-15b, and *rac*-15e

General Features. Single-crystal X-ray structural determinations were carried out on selected *ansa*-lanthanidocene amide complexes in order to unambiguously establish the C_2 symmetry of the bis(indenyl) complexes and to detect any systematic structural features. For ease of comparison, key parameters of the metallocene amide complexes are listed in Table 2. Details of the ligand framework are described by several angles between selected planes and compared to relevant data from the literature (Figure 5, Table 3).

All of the complexes display an almost perfect trigonal planar arrangement of the amide and the *ansa*-ligand. The C_g−Ln−C_g angle increases slightly with decreasing cation size (C_g is the center of the five-membered ring). In all of the molecular structures, both of the Si−H moieties approach the Ln(III) center in an agostic manner. So far, it was the asymmetric, monoagostic approach of one $SiMe_3$ moiety exclusively which has been found in heteroleptic metallocene complexes carrying silylamide as well as silylated hydrocarbon substituents.[9,44−46] Although this series of *ansa*-metallocene complexes exhibits a similar molecular coordination geometry, both *ansa*-ligand and metal variation have significant implications for the β-SiH agostic interaction of the silylamide fragment. The present close Ln···Si contacts ranging from 3.028(1) to 3.246(1) Å already resemble Ln−Si σ-bond distances,[47] suggesting an appreciable interaction in the solid state, which remains in solution, as indicated by the spectroscopic investigations discussed above. Additionally, close Ln···H contacts[48] (2.38(3)−2.70(3) Å) at the upper end of covalent Ln−H bonds[49] complete the formation of agostically fused Ln−N−Si−H four-membered rings. These rings display only small torsional angles (1(1)−6(1)°) and are located in a plane almost parallel to the bisector of the two

(44) Stern, D.; Sabat, M.; Marks, T. J. *J. Am. Chem. Soc.* **1990**, *112*, 9558−9575.

(45) In theoretical studies the asymmetric geometry has been attributed to an interaction between the electron-deficient Ln(III) center and the electron density of the Si−C bond: (a) Tatsumi, K.; Nakamura, A. *J. Am. Chem. Soc.* **1987**, *109*, 3195−3206. (b) Bursten, B. E.; Fang, A. *Inorg. Chim. Acta* **1985**, *110*, 153−160.

(46) Correspondingly, the interactions discussed in this paper involve the electron density of the SiH fragment: Scherer, W. Ph.D. Thesis, Technische Universität München, 1993.

(47) (a) A comparable Sm−Si distance of 3.0524(8) Å was reported for $Cp^*_2Sm[SiH(SiMe_3)_2]$: Radu, N. S.; Tilley, T. D.; Rheingold, A. L. *J. Am. Chem. Soc.* **1992**, *114*, 8293−8295. (b) $(Me_3SiCH_2)Y[(\mu\text{-}(CH_2)_2SiMe_2][(\mu\text{-}OCH_3)Li(thf)_2]_2$ reveals a Y−Si distance of 3.147(2) Å: Evans, W. J.; Boyle, T. J.; Ziller, W. J. *J. Organomet. Chem.* **1993**, *462*, 141−148.

(48) All SiH hydrogens atoms were located in difference Fourier maps and successfully refined. Of course, the usual caution regarding the accuracy of hydrogen positions in heavy atom structures was applied. In fact, though a lengthening of the agostically interacting Si−H bonds should be expected, the refined SiH positions yield bond lengths of 1.43−1.47 Å, which are even shorter than normal SiH distances in hydrosilanes (1.47−1.50 Å; Lukevics, E.; Pudowa, O.; Sturkovich, R. *Molecular Structure of Organosilicon Compounds*; Ellis-Horwood: Chichester, U.K., 1989).

Table 3. Selection of Twisted Geometry Parameters (deg) for Lanthanidocene Amide and Comparable Complexes

compound	α^a	β^a	γ^a	Ω^a	Θ^a
11c	102.8(1)	16.6(2)/18.1(2)	−	68.2(2)	2.56(8)
rac-**13b**	100.9(1)	19.9(2)	1.8(2)	61.2(2)	5.31(9)
rac-**13e**	99.7(2)	19.8(2)	1.5(2)	59.7(2)	4.5(2)
rac-**15b**	98.7(2)	17.9(2)/17.6(2)	5.5(2)/4.9(2)	66.0(1)	7.74(9)
rac-**15e**	98.1(3)	18.5(3)/18.6(3)	5.3(3)/2.3(3)	65.6(2)	11.0(7)
rac-**12b**(THF) (ref 23)	103.1(2)	12.3(2)/12.3(2)	3.0(2)/4.1(1)	82.5(1)	45.8(3)
$[Me2Si(Cp^{Menthyl})_2]Y-N(SiMe_3)_2$ (ref 27)	98.2	16.6/15.8	−	66.1/69.2	6.7/15.0
$Cp^*_2YN(SiMe_3)_2$ (ref 50)	−	15.5	−	45.2	−
$(C_5H_4Et)_2YN(SiMe_3)_2$ (ref 51)	−	14.7	−	47.19	−
$\{[Me_2Si(Cp'')_2]ThH_2\}_2$ (ref 52)	102.6/98.5	13.1/16.2 11.2/16.8	−	73.3/70.6	−[b]
$[Me_2Si(2\text{-}Me\text{-}Ind)_2]ZrCl_2$ (ref 25b)	94.4	17.4/16.8	2.6/5.0	60.2	1.3
$[Me_2Si(2\text{-}Me\text{-}Benz\text{-}Ind)_2]ZrCl_2$ (ref 25c)	94.8	17.0	1.7	61.6	0.8

[a] For angle definitions see Figure 5. [b] No hydrogen atom positions available.

cyclopentadienyl and indenyl rings, respectively. The strong symmetric Ln···SiH interaction causes extremely widened Si−N−Si angles (144.0(2)−160.1(2)°) and a concomitant significant contraction of both Ln−N−Si angles (99.5(2)−108.0(1)°); the range observed for the amide precursors **7** is 109.0(3)−123.2(2)°.[16] The two methyl groups of each silylamide silicon atom are mirrored by the Si−N−Si plane. Interestingly, the lutetium complex *rac*-**15e** features a slightly perturbated silylamide coordination, probably as a result of peculiar steric constraints (vide infra).

Details of the Molecular Structures. Compound $[Me_2Si(Cp'')_2]La[N(SiHMe_2)_2]$ (**11c**) crystallizes in the triclinic space group $P\bar{1}$. The C_2-symmetric *ansa*-indenyl compounds exhibit centrosymmetric unit cells of *C*2/*c* symmetry for the homologous *ansa*-metallocenes *rac*-**13b** and *rac*-**13e** and of $P\bar{1}$ symmetry for *rac*-**15b** and *rac*-**15e**, respectively.

The molecular structure of the C_{2v}-symmetric complex **11c** (Figure 6) resembles those of the numerous structurally characterized complexes of type "Cp_2LnX", in particular that of $Cp^*_2Y[N(SiMe_3)_2]$,[50] adopting the typical bent metallocene arrangement.[9] The La−C distances range from 2.738(2) to 2.786(7) Å, the *ipso*-carbon atom being the closest to the La(III) cation. The cyclopentadienyl rings are tilted against the Si3−C_{ipso} axis toward the metal center (β = 16.6(2)°/18.1(2)°), while the C_{ipso}−Si3−C_{ipso} angle is only slightly contracted (α = 102.8(1)°) (Figure 5 and Table 3). Such a "U-shaped" ($\beta \gg 0$) coordination of the linked cyclopentadienyl ligand seems to be directed by the large metal center. These angle distortions generate an *ipso* carbon atom of enhanced sp^3-character. In comparable actinide and zirconocene complexes, the deviation of the "V-shaped" ($\beta \approx 0$) ligand coordination appears less pronounced (Table 3). The smaller Zr(IV) centers can be accommodated by *ansa*-ligands via a more contracted angle α (94.4−94.8°) and a comparable tilt angle β (16.8−17.4°),[25b,c] whereas the larger Th(IV) complex displays tentatively less tilted cyclopentadienyl planes (β = 11.2−16.8°).[52,53]

Despite the distinctly U-shaped *ansa*-ligand in **11c**, the large lanthanum cation forces a large bite angle Ω of 68.2(2)°, which is exceeded only by those of complex $\{[Me_2Si(Cp'')_2]ThH_2\}_2$[52] ($\Omega$ = 73.3/70.6°) and the propylidene-bridged *ansa*-complex *rac*-**12b**(THF) (Ω = 82.5).[23] Such large bite angles are assumed to facilitate the diagostic approach of the dimethylsilylamide moiety to the Lewis acidic metal ion. The La−N bond length of 2.449(3) Å compares well with the La−N distances in nine-coordinated $[Cp^*_2La][\mu\text{-}(C_{12}H_8N_2)]$ (2.452(2) Å)[54] and appears markedly elongated compared to those in eight-coordinated complex $Cp^*_2La(NHMe)(H_2NMe)$ (2.32(1) Å)[55] and its five-coordinated synthetic precursor (2.395(5)−2.416(5) Å).[15] The La−Si (3.2460(9)/3.2440(9) Å) and La−H (2.70(3)/2.66(4) Å) contacts are slightly elongated compared to those of σ-bonded silicon[47] and bridging hydride ligands,[49] respectively, taking into

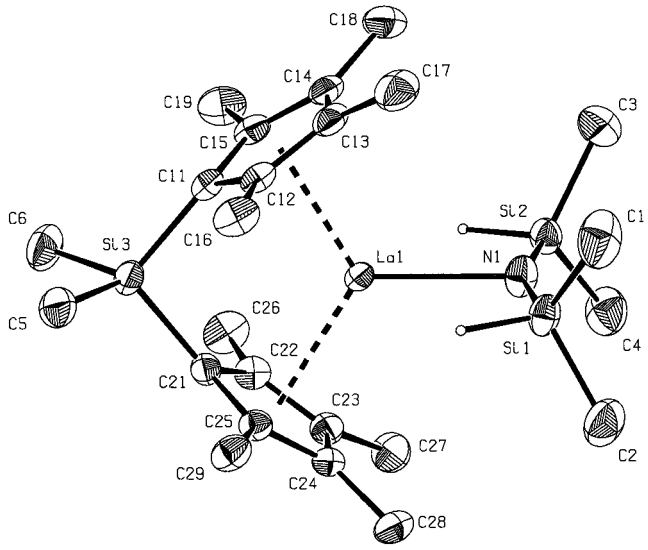

Figure 6. PLATON[80] drawing of **11c**. Atoms are represented by thermal ellipsoids at the 50% level. Except for H(1) and H(2), all hydrogen atoms are omitted for clarity. For selected distances and angles, see Tables 2 and 3.

(49) Examples of Ln−H bond lengths from X-ray diffraction data include the following. (a) 2.19/2.17 Å in $[(C_5H_4Me)_2Y(\mu\text{-}H)(THF)]_2$: Evans, W. J.; Meadows, J. H.; Wayda, A. L.; Hunter, W. E.; Atwood, J. L. *J. Am. Chem. Soc.* **1982**, *106*, 2008−2014. (b) 2.35 Å in $[(C_5H_5)_2Y(\mu\text{-}Cl)]_2(\mu\text{-}H)\text{-}AlH_2(OEt_2)$: Lobovskii, B.; Soloveichik, G. L.; Erofeev, A. B.; Bulichev, B. M.; Bel'skii, V. K. *J. Organomet. Chem.* **1982**, *235*, 151−158. (c) 1.98/2.13 Å in $[(C_5H_5)_2Lu(\mu\text{-}H)(THF)]_2$: Schumann, H.; Genthe, W.; Hahn, E.; Hossain, M. B.; van der Helm, D. *J. Organomet. Chem.* **1986**, *299*, 67−84. (d) 2.59/2.25/2.29 Å in $[(BH_3)_2La(THF)_5][(BH_3)_4La(THF)_2]$: Bel'skii, V. K.; Sobolev, A. N.; Bulychev, B. M.; Alikhanova, T. Kh.; Kurbonbekov, A.; Mirsaidov, U. *Koord. Khim.* **1990**, *16*, 1963−1969.

(50) Den Haan, K. H.; De Boer, J. L.; Teuben, J. H.; Speck, A. L.; Kojic-Prodic, B.; Hays, G. R.; Huis, R. *Organometallics* **1986**, *5*, 1726−1733.

(51) Schumann, H.; Rosenthal, E. C. E.; Kociok-Köhn, G.; Molander, G. A.; Winterfeld, J. *J. Organomet. Chem.* **1995**, *496*, 233−240.

(52) Fendrick, C. M.; Schertz, L. D.; Day, V. W.; Marks, T. J. *Organometallics* **1988**, *7*, 1828−1839.

(53) The more covalent dimethylsilyl-bridged ferrocenyl complexes exhibit tilt angles β as large as 40.0°, affording a nearly planar arrangement of both cyclopentadienyl rings: (a) Rulhuns, R.; Lough, A. J.; Mannus, I. *Angew. Chem.* **1996**, *108*, 1929−1931; *Angew. Chem., Int. Ed. Engl.* **1996**, *35*, 1805−1807. (b) Herberhold, M.; Steffl, U.; Milius, W.; Wrackmeyer, B. *Angew. Chem.* **1996**, *108*, 1927−1929; *Angew. Chem., Int. Ed. Engl.* **1996**, *35*, 1863−1864. (c) Stoeckli-Evans, H.; Osborne, A. G.; Whiteley, R. H. *Helv. Chim. Acta* **1976**, *59*, 2402−2406.

(54) Scholz, J.; Scholz, A.; Weimann, R.; Janiak, C.; Schumann, H. *Angew. Chem.* **1994**, *106*, 1220−1223; *Angew. Chem., Int. Ed. Engl.* **1994**, *33*, 1171−1174.

(55) Gagne, M. R.; Stern, C. L.; Marks, T. J. *J. Am. Chem. Soc.* **1992**, *114*, 275−294.

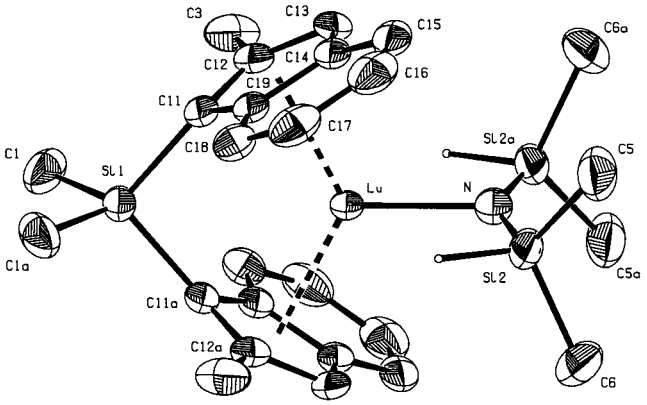

Figure 7. PLATON[80] drawing of *rac*-**13e**. Atoms are represented by thermal ellipsoids at the 30% level. Except for H(2) and H(2a), all hydrogen atoms are omitted for clarity. For selected distances and angles see Tables 2 and 3. *rac*-**13b** is isostructural.[14]

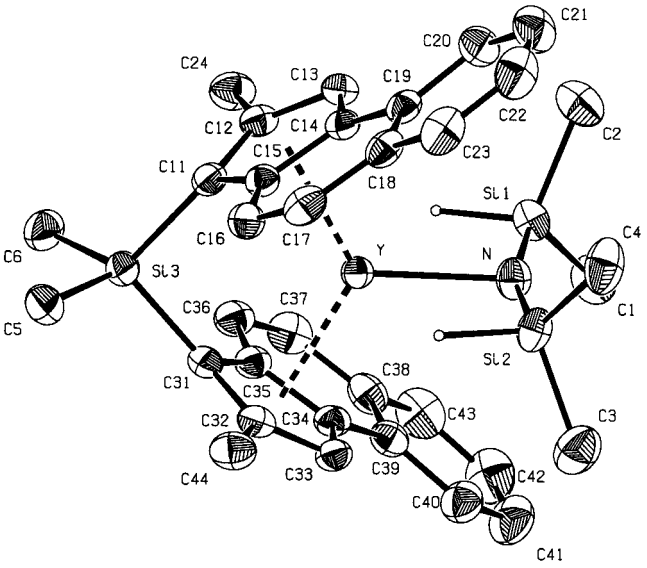

Figure 8. PLATON[80] drawing of *rac*-**15b**. Atoms are represented by thermal ellipsoides at the 50% level. Except for H(1) and H(2), all hydrogen atoms are omitted for clarity. For selected distances and angles see Tables 2 and 3.

account the different cation size and coordination number.[56] Similar bonding parameters were recently detected in the single-crystal neutron diffraction structures of the *monoagostic* complex Cp*La[CH(SiMe$_3$)$_2$]$_2$ (La···Si, 3.35(1)−3.42(1) Å)[57] and the *polyagostic* complex Nd[AlMe$_4$]$_3$(Al$_2$Me$_6$)$_{0.5}$ (Nd···H, 2.65(1) Å).[58a]

The X-ray structure analyses of the bis(indenyl) complexes *rac*-**13b**, *rac*-**13e**, *rac*-**15b**, and *rac*-**15e** reveal the *trans*-coordination of the chelating ligands, which determines the C_2 symmetry of the thermodynamically more favorable *rac*-complexes as presented in Figures 7−9. Their overall geometry is analogous to that of the C_{2v}-symmetric metallocene amide **11c**. The Y−C and Lu−C bond distances lie in the expected range; however, the π-ancillary ligation of the benzoindenyl system shows considerable distortions (ΔLn−C$_{Cp}$ = 0.07−0.11 Å). The Y−N bond distances in *rac*-**13b** (2.237(4) Å) and *rac*-

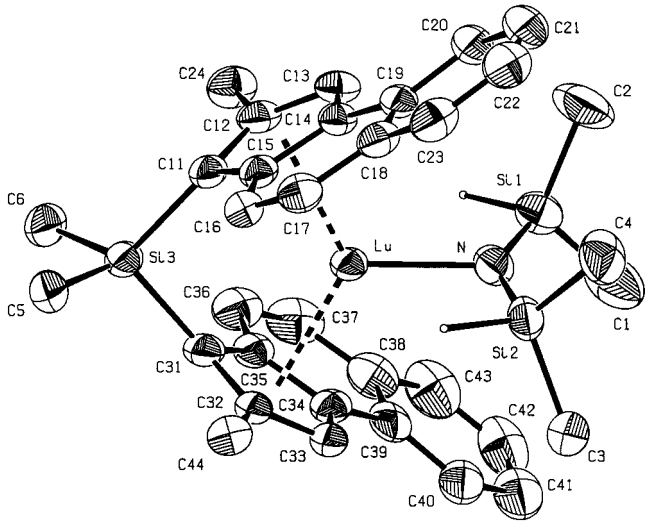

Figure 9. PLATON[80] drawing of *rac*-**15e**. Atoms are represented by thermal ellipsoids at the 30% level. Except for H(1) and H(2), all hydrogen atoms are omitted for clarity. For selected distances and angles see Tables 2 and 3.

15b (2.274(3) Å) correlate well with the corresponding distances in seven-coordinated yttrium amide complexes, e.g., Cp*$_2$-Y[N(SiMe$_3$)$_2$] (2.274(5) Å) and {(*R*)-Me$_2$Si(Me$_4$C$_5$)[(−)-menthyl-C$_5$H$_3$]}Y[N(SiMe$_3$)$_2$] (2.211(8), 2.281(8) Å).[44,50] Remarkably, complex *rac*-**13e** features a Lu−N bond length of 2.159(4) Å, which is even shorter than that in the five-coordinate amide precursor (**7e**, 2.184(3)−2.238(3) Å). The shortest Ln−N bond reported so far was observed in the polyagostic complex Nd(N*i*Pr$_2$)[(μ-Me)(μ-N*i*Pr$_2$)AlMe$_2$][(μ-Me)$_2$AlMe$_2$] (2.168(2) Å).[58b]

The present geometrical parameters depend on the cation size and the type of *ansa*-ligand. Complexes *rac*-**13b** and *rac*-**13e** display bite angles Ω (61.2(1)°, 59.7(2)°) in the range of those of related zirconocene complexes.[25b,c] For comparison, the bite angles present in nonlinked cyclopentadienyl and indene derivatives Cp*$_2$Y[N(SiMe$_3$)$_2$],[50] (C$_5$Me$_4$Et)$_2$Y[N(SiMe$_3$)$_2$],[51] and [(2,4,7-Me$_3$C$_9$H$_4$)$_2$Y(μ-H)]$_2$[12e] are considerably smaller (45.2/47.2/46.6/47.8°).[50] The molecular structures of the benzoindenyl-derived complexes *rac*-**15b** and *rac*-**15e** show relatively large bite angles of 66.0(1)° and 65.6(2)°, respectively, comparable to that of the lanthanum complex **11c**. Additionally, small but significant differences of the geometrical parameters β, γ, and Θ (Table 3) are detected for the *rac*-derivatives of complexes **13** and **15**. The comparatively slightly decreased (β) and increased (γ, Θ) values in complexes **15** are probably due to the steric interaction of the silylamide moiety with the 4,5-benzo substituents. Particularly, the latter parameters γ and Θ defining the curvature of the aromatic system away from the silyl groups of the amide (*rac*-**15b**, γ = 5.5(2)/4.9(2)°; *rac*-**15e**, 5.3(3)/2.3(3)) and the distortion of the silylamide plane (Θ = 7.7(1)°, 11.0(7)°), respectively, exceed the values of the related zirconium complex [Me$_2$Si(2-Me-Benz-Ind)$_2$]ZrCl$_2$.[25c]

The Si−N−Si angle deformation detected in the [N(SiHMe$_2$)$_2$] moiety originates from the strong diagostic interaction; however, there seems to be no clear correlation between the cation size and this intrinsic enlargement of the Si−N−Si angles. The agostic Ln−Si and Ln−H distances decrease in the order **11c** (La) > *rac*-**13e** (Lu) > *rac*-**13b** (Y) > *rac*-**15b** (Y) and are in the range of covalent bonds for the latter one.[47,48] The angle of 153.3(2)° in *rac*-**13b** is only slightly smaller than that of **11c**, ranging between those of *rac*-**13e** (144.0(2)°) and *rac*-**15b** (160.1(2)°). This angle expansion appears to be limited mainly by steric interaction between the SiMe$_2$H groups and

(56) Shannon, R. D. *Acta Crystallogr.* **1976**, *A32*, 751−767.
(57) Klooster, W. T.; Brammer, L.; Schaverien, C. J.; Budzelaar, P. H. M. *J. Am. Chem. Soc.* **1999**, *121*, 1381−1382.
(58) (a) Klooster, W. T.; Lu, R. S.; Anwander, R.; Evans, W. J.; Koetzle, T. F.; Bau, R. *Angew. Chem.* **1998**, *110*, 1326−1329; *Angew. Chem., Int. Ed. Engl.* **1998**, *37*, 1268−1270. (b) Evans, B. J.; Anwander, R.; Ziller, J. W.; Khan, S. I. *Inorg. Chem.* **1995**, *34*, 5927−5930.

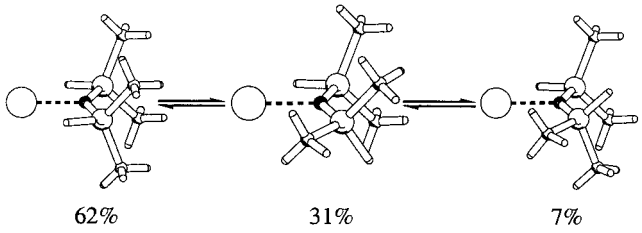

Figure 10. Disordering model of the silylamide moiety in *rac*-**15e**.

the *ansa*-ligand framework: the closest distance[59] measured between the amide moiety and the hydrogen atoms of the aromatic systems are almost equal for all of the complexes and just slightly below the sum of the van der Waals radii (**11c**, 1.96 Å; *rac*-**13b**, 2.16 Å; *rac*-**13e**, 2.24 Å; *rac*-**15b**, 2.10 Å; *rac*-**15e**, 2.18 Å). For example, the bis(indenyl) complexes feature the closest contact between the C3−H hydrogen and the corresponding methylsilyl group. The interaction of the silylamide moiety with the 4,5-benzo substituent is particularly pronounced in complex *rac*-**15e**, as revealed by the comparatively long Lu−N bond distance of 2.173(5) Å and a crystallographically disordered $SiHMe_2$ moiety (Figure 10). Extended embedding of the smaller lutetium center into the ligand bite sterically disfavors a strong β-SiH diagostic interaction, which would cause an increased interaction of the methyl groups of the silylamide ligand and the 2-Me substituent of the *ansa*-system. To reduce a sterically stressed, staggered conformation of the $SiHMe_2$ groups, rotation about the Si−N bond occurs. This peculiar situation is expressed in the extreme values of γ (5.3(3)°/2.3(3)°) and θ (11.0(7)°) and a comparatively small Si−N−Si angle of 139.3(4)°.

A correlation between Si−N−Si angles and their pertinent Si−N distances reveals that the electronic situation in the agostically tensioned bis(dimethylsilyl)amide fragments cannot be described in terms of a simple rehybridization model only (Figure 11).

All of the nonmetallocene bis(dimethylsilyl)amide moieties approximately fit one function (plot A), as derived from a hybridization model.[60] Although the Si−N−Si angles exhibit enhanced flexibility, the data from both μ_1- and μ_2-coordinated bis(dimethylsilyl)amide fragments fit considerably well. The angle/distance correlation of the *ansa*-metallocene silylamide complexes described herein can be fitted by a second, steeper plot B. It is only the disordered $SiHMe_2$ moiety of complex *rac*-**15e** which significantly deviates from this plot B, even approaching plot A. Apparently, these complexes experience no significant change of hybridization at the nitrogen atom: the Si−N distances remain comparable to the educt amide

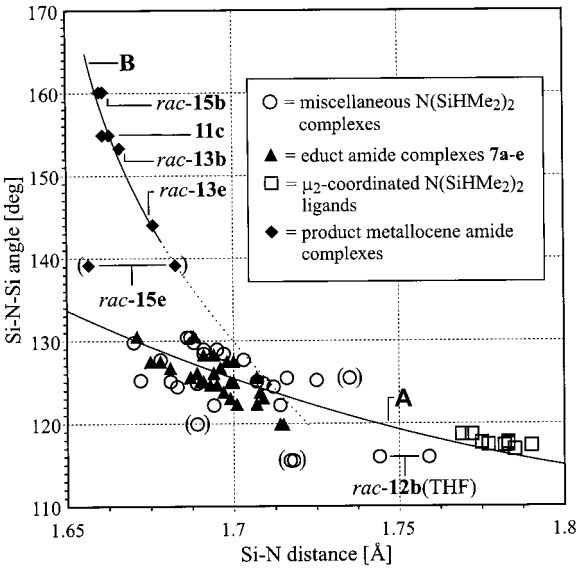

Figure 11. Correlation between Si−N−Si angles and their pertinent Si−N distances in bis(dimethylsilyl)amide complexes. The correlation functions[57b] were derived from a hybridization model. Data points in parentheses result from disordered bis(dimethylsilyl)amide moieties and were not taken into account for fitting the functions.

complexes (**7a**−**e**) when the Si−N−Si angle is enlarged. Therefore, it can be assumed that the observed Si−H diagostic interaction not only is due to an attractive interaction between the silicon hydrogen atoms and the metal center but also affects the electron distribution of the entire silylamide ligand.

So far, the question remained unsolved of why these *ansa*-metallocene complexes do not show the usually observed agostic interaction of one silyl group of the amide ligand (Figure 12b)[44,50,51,57] but display this unique symmetric approach of both SiH moieties (Figure 12a).[58,61,62] According to theoretical calculations,[22] the present agostic interaction is mainly ionic, taking place via the attraction of the negative partial charge of the SiH hydrogen atoms and the Lewis acidic Ln(III) metal centers. However, covalent bonding contributions cannot be neglected, as revealed by the peculiar behavior of the SiH group in spectroscopic examinations. Such a diagostic interaction leads to a significant decrease of the molecule's total energy, with the Si−N−Si angle deformation energy of 0.1−1.0 kcal/mol being compensated by the β-SiH diagostic interaction, which can be estimated as 6.4 kcal/mol.[22]

Kinetic and Thermodynamic Limitations of the Extended Silylamide Route

General Considerations. The synthetic yields of the *ansa*-lanthanidocene complexes presented in Scheme 1 markedly depend on the nature of the chelating ligand. For example, the low reactivity of the 2,4-substituted bis(indene) **4** is in contrast to the high crystallized racemic yields obtained for the similarly bulky bis(benzoindene) **5**. In the following, both thermodynamic and kinetic limitations of this extended silylamide route are addressed on the basis of pK_a and steric factors. Amine elimination reactions as described in Schemes 1 and 2 represent

(59) As hydrogen atom locations on the basis of X-ray data are not very reliable, the closest possible distances were calculated by a simple trigonometric approach, assuming free rotation of the CH_3 groups around their bond axis. Calculations were done on the basis of the observed C−C distances, combined with the following neutron diffraction data for hydrogen atoms: C_{alkyl}−H = 1.113 Å; C_{aromat}−H = 1.090 Å; ∠H−C−Si = 107°. The hydrogen atoms of the aromatic systems were placed on the bisector of the C−CH−C angles.

(60) (a) The correlation between the Si−N−Si angles and the pertinent Si−N distances was based on 72 data points, taken from 17 compounds (data sources: CSD, refs 15, 16 and this publication). (b) Assuming a linear correlation of the p-orbital content P in the sp^n hybrid and the Si−N distance d ($d = S(0) + kP$), from $\cos\alpha = (P - 1)/P$ (α = Si−N−Si angle) the correlation function $d = S(0) + k/(1 - \cos\alpha)$ can be obtained. This function was fitted to the data points by least-squares refinement. The resulting parameters are, for the metallocene silylamides, $S(0) = 1.440$ and $k = 0.425$ (rms = 0.0132) and, for unperturbated monoagostic silylamides, $S(0) = 1.300$, $k = 0.881$ (rms = 0.0154). For $180° > \alpha > 90°$, theoretical Si−N bond distances in the range $1.653 < d < 1.866$ Å and $1.530 < d < 2.179$ Å can be derived for metallocene silylamide complexes and for unperturbated silylamide complexes, respectively.

(61) A diagostic interaction of a bis(dimethylsilyl)alkyl moiety has been described recently: Sekiguchi, A.; Ichnohe, M.; Takahashi, M.; Kabuto, C.; Sahurai, H. *Angew. Chem.* **1997**, *109*, 1577−1579; *Angew. Chem., Int. Ed. Engl.* **1997**, *36*, 1533−1534. In contrast to the interactions described by us, this β-SiH diagostic interaction involves two different metal centers, Li^+ cations, and hence insignificantly increased Si−C−Si angles.

(62) For polyagostic Ln···Me interactions, see: Tilley, T. D.; Andersen, R. A.; Zalkin, A. *Inorg. Chem.* **1984**, *23*, 2271−2276.

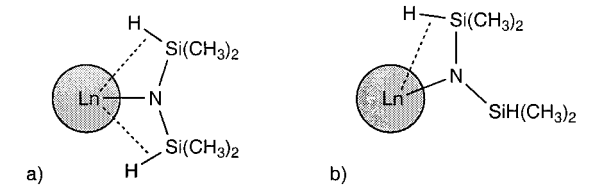

Figure 12. Symmetric (a) and asymmetric (b) coordination mode of the silylamide moiety.

Scheme 3. Reaction Mechanism Proposed for the Formation of *ansa*-Metallocene Amide Complex **11b** via the Extended Silylamide Route Based on the Isolated Intermediates **17b** and **14b**

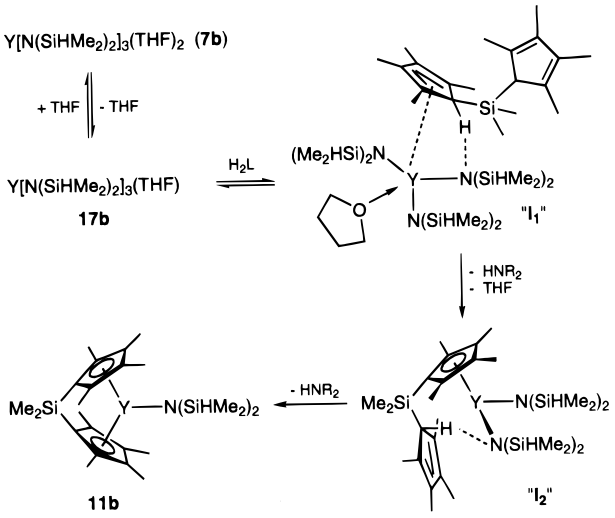

Brönsted-type acid−base reactions, the approach of the protic substrate and subsequent proton transfer to the amide nitrogen being the key steps of the reaction. Hence, the thermodynamics of the exchange reactions can be best understood by determining the pK_a values of the ligands involved. Factors such as steric oversaturation/unsaturation are known to govern the feasibility of ligand-exchange reactions in rare earth chemistry.[16] The isolation of the reaction intermediates **14b** and **17b** substantiates the presence of kinetically controlled exchange reactions under the prevailing conditions and proposes a reaction mechanism such as that depicted in Scheme 3. Unsuccessful or incomplete exchange reactions utilizing the sterically more crowded Ln[N(SiMe$_3$)$_2$]$_3$ complexes reinforce this mechanistic scenario.

The exchange reaction is initiated by THF dissociation from the amide precursor, affording, e.g., the mono-THF adduct Ln[N(SiHMe$_2$)$_2$]$_3$(THF) (**17**). The yttrium derivative **17b** was obtained independently by refluxing **7b** in toluene and characterized spectroscopically and by elemental analysis. The unoccupied coordination site in complex **17b** directs approach and coordination of one "diene" moiety of the linked cyclopentadienyl ligands to give intermediate $\mathbf{I_1}$. After transfer of the "acidic" proton onto the amide nitrogen, dissociation of the protonated silylamine and of the second THF molecule results in a reaction intermediate $\mathbf{I_2}$ comparable to complex **14b**. The final ligand association proceeds via the second proton transfer, followed by displacement of the amine by the chelating ligand. On the basis of this mechanism, two key limitations of the exchange reactions are evident. First, the presence of the dissociated THF donor molecule should slow the reactivity, as it can be coordinated on each step of product formation and thus block coordination sites. Second, the steric bulk of the approaching protic molecule restricts the ligand orientation for the following proton transfer.

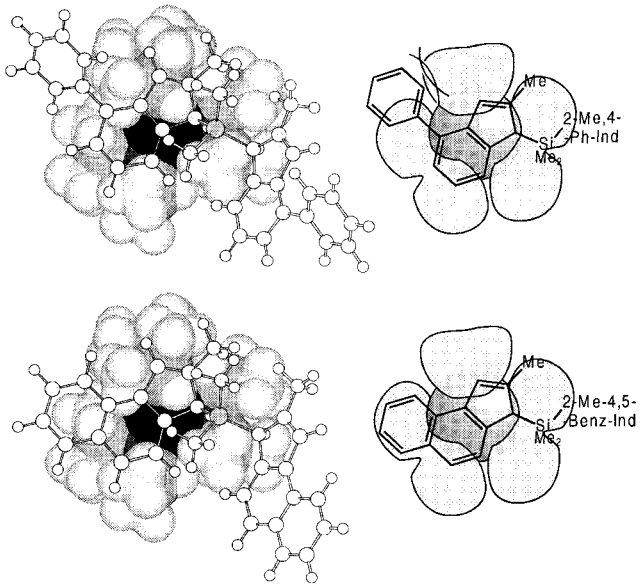

Figure 13. Sterically hindered (above) and unhindered (below) approach of 2,4-substituted *ansa*-indene molecules **4** and **5**, respectively, at complex Ln[N(SiHMe$_2$)$_2$]$_3$(THF) on the basis of MM2 calculations.

Kinetically Controlled Ligand Approach. A qualitative description of the implications of steric hindrance for this specialized silylamine elimination could be gained on the basis of MM2 force field calculations. According to the mechanism proposed above (Scheme 3), ligand approach at the mono-THF adduct **17b** was chosen as a model reaction. The calculated geometry of reaction intermediate **17b** is in good accordance with that of the mono-dimethylimidazol-2-ylidene adduct Y[N(SiHMe$_2$)$_2$]$_3$(Me$_2$C$_3$H$_2$N$_2$) reported recently.[63]

Approach of the differently substituted linked bis(indenes) **4** and **5** was forced by a fixed C−H···N distance of 3.20 Å.[64] The resulting structure of reaction intermediate $\mathbf{I}_1$ clearly shows that steric constraints hamper the proton exchange process (Figure 13). The pincers formed by the methyl and phenyl substituents in the 2- and 4-positions are too small to match the bulk of the bis(dimethylsilyl)amide ligand. In contrast, the 4,5-benzo-substituted bis(indene) seems to perfectly fit into the void which is formed by the amide ligands of **17b**. These findings are in good accordance with the synthetic results, which show a high crystallized yield for complexes **15** and no or incomplete ligand exchange for complexes **14**.

pK_a Value Estimation. Many pK_a value estimations have been carried out for amines and hydrocarbons which resulted in a number of different pK_a scales, depending on the applied solvent, the counterions, and the method of measurement.[65−67] The method introduced by Fraser et al.[65] comprises an acidity scale which seemed to be well suited to evaluate our extended silylamide route. According to these studies, ^{13}C NMR spectroscopy is used to measure the relative concentrations of all four species of a deprotonation/reprotonation equilibrium, as shown in Scheme 4.

(63) Herrmann, W. A.; Munck, F. C.; Artus, G. R. J.; Runte, O.; Anwander, R. *Organometallics* **1997**, *16*, 682−688.

(64) So far, few C−H···N distances have been reported. A relatively strong C−H···N hydrogen bond in methylnitrile results in a close C···N contact of 318 pm: Dulmage, W. J.; Lipscomb, W. N. *Acta Crystallogr.* **1951**, *4*, 330−335. For a recent discussion, see: Mascal, M. *Chem. Commun.* **1998**, 303−304.

(65) (a) Fraser, R. R.; Besse, M.; Mansour, T. S. *J. Chem. Soc., Chem. Commun.* **1983**, 620−621. (b) Fraser, R. R.; Mansour, T. S.; Savard, S. *J. Org. Chem.* **1985**, *50*, 3232−3234. (c) Fraser, R. R.; Mansour, T. S.; Savard, S. *Can. J. Chem.* **1985**, *63*, 3505−3509 and references therein.

Scheme 4. pK_a Value Estimation by the Method of Fraser et al.[65]

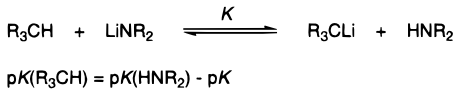

However, application of this method to silyl-bridged bis(indene) and bis(fluorene) systems is hampered by different effects. Donor solvent-dependent equilibria between solvent separated (ssip) and contact ion pairs (cip) (a),[68] different solvation and coordination isomers of the dilithium salts of chelating ligands present in solution (b),[69] disproportionation equilibria between mono- and bis-deprotonated species with the neutral ligand (c), and 1,5-sigmatropic shifts of the silyl group (d)[70] contribute to signal broadening and/or signal multiplicities and hence often result in noninterpretable spectra (Scheme 5).

To minimize these aggravating factors, monosilylated indene and fluorene systems **8a**−**10a** were used for the pK_a value determinations. The new compounds were synthesized by silylation of the corresponding lithium salts with dimethylchlorosilane as shown in Scheme 6.[71] A further simplification of the system could be achieved by recording the spectra in a solvent mixture of C_6D_6/THF-d_8 (20/1), which resembles the conditions of the extended silylamide route and counteracts ssip formation. Silyl group shift reactions proved to be negligible: according to the ^{1}H NMR spectrum of **8a**, in addition to the thermodynamically favored 3-(dimethylsilyl)indene (94%) only a small amount of the 1-substituted derivative (6%) formed. Such small amounts are below the accuracy of the estimation of ^{13}C NMR signal intensities and therefore hardly affect the determination of the pK_a values. The pK_a values estimated by this modification of the method of Fraser et al. are presented in Table 4.

Scheme 5. Problems Associated with pK_a Value Estimations: (a) ssip/cip Equilibrium, (b) Solvation and Coordination Isomers of the Li^+, (c) Mono- and Bis-deprotonation of the *ansa*-Ligand, and (d) Migration of the Silyl Group

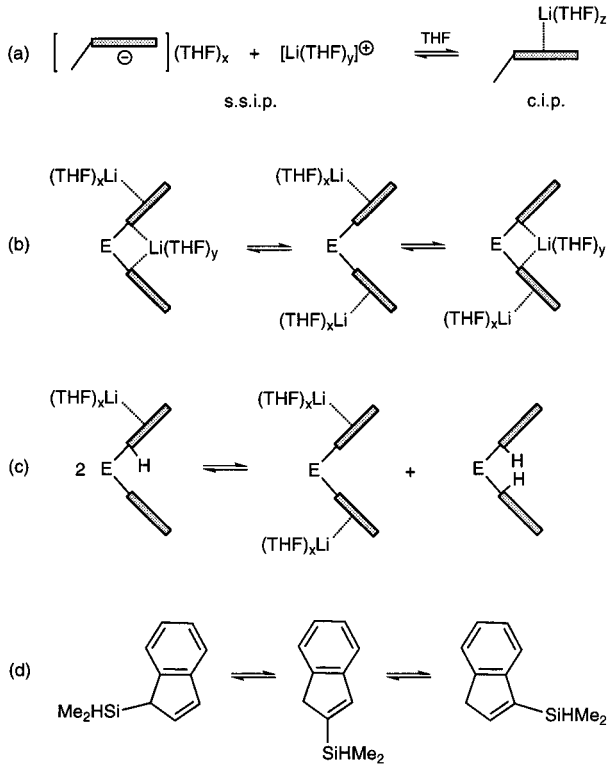

Scheme 6. Preparation of Silylated Indene and Fluorene Model Compounds for the pK_a Value Estimation

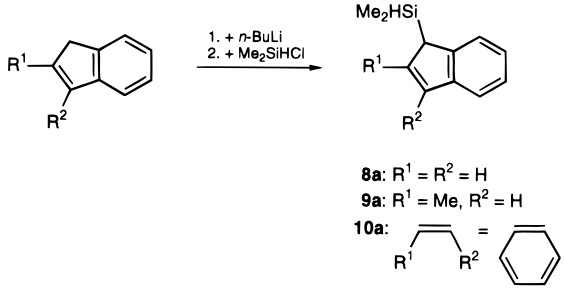

Silylamines display a relatively low basicity attributable to dπ−pπ interactions between the vacant d-orbitals of the silicon atoms and the lone pairs of the amide nitrogen.[72] For example, the pK_a value of the bis(trimethylsilyl)amine was determined as 25.8 in THF.[65b] According to our estimations, the pK_a of bis(dimethylsilyl)amine is as low as 22.8.[73] Three differently performed acidity measurements of fluorene (runs 2, 3, and 5) demonstrate the accuracy of this method. Variation of the reference acids, the pK_a values of which were determined first (runs 1 and 4), resulted in pK_a values varying within 0.1 unit. Generally, the present values are about 1.5 units higher than the ones obtained by other methods in DMSO. The presence of a silyl group in the 3-position decreases the pK_a value by 1.5 and 1.8 units for the indenyl derivatives **8a** and **9a**, respectively.

(66) For reviews about pK_a value estimations, see: (a) Streitwieser, A., Jr.; Juaristi, E.; Nebenzahl L. L. In *Comprehensive carbanion chemistry, Part A*; Buncel, E., Durst, T., Eds.; Elsevier-North Holland: Amsterdam, 1980; pp 323−382. (b) Reutov, O. A.; Beletskaya, I. P.; Butin, K. P. *CH-Acids*; Pergamon Press: Oxford, 1978. (c) For recent advances in measurement techniques, see: Bausch, M. J.; Gong, Y. *J. Am. Chem. Soc.* **1994**, *116*, 5963−5964. (d) Bordwell, F. G.; Cheng, P.-J.; Ji, G.-Z.; Satish, A. V.; Zhang, X. *J. Am. Chem. Soc.* **1991**, *113*, 9790−9795. (e) Streitwieser, A.; Ciula, J. C.; Krom, J. A.; Thiele, G. *J. Org. Chem.* **1991**, *56*, 1074−1076.

(67) Matthews, W. A.; Bares, J. E.; Bartmess, J. E.; Bordwell, F. G.; Cornforth, F. J.; Drucker, G. E.; Magolin, Z.; McCallum, R. J.; Mc. Collum, G. J., Vanier, N. R. *J. Am. Chem. Soc.* **1975**, *97*, 7006−7014.

(68) For discussions of ssip/cip equilibria, see refs 62a,b and the following: (a) O'Brien, D. H. In *Comprehensive carbanion chemistry, Part A*; Buncel, E., Durst, T., Eds.; Elsevier-North Holland: Amsterdam, 1980; pp 271−322. (b) Eiermann, M.; Hafner, K. *J. Am. Chem. Soc.* **1992**, *114*, 135−140. (c) O'Brian, H. D.; Russel, R. C.; Hart, A. J. *J. Am. Chem. Soc.* **1979**, *101*, 633−639. (d) Grutzner, J. B.; Lawlor, J. M.; Jackman, L. M. *J. Am. Chem. Soc.* **1972**, *64*, 2306−2314.

(69) Harder, S.; Lutz, M.; Straub, A. W. G. *Organometallics* **1997**, *177*, 107−113.

(70) 1,5-Sigmatropic shifts of silyl groups at cyclopentadienyl and indenyl systems are well established in the literature. For recent examples, see: (a) Stradiotto, M.; Rigby, S. S.; Hughes, D. W.; Brook, M. A.; Bain, A. D.; McGlinchey, M. J. *Organometallics* **1996**, *15*, 5645−5652. (b) Rigby, S. S.; Gupta, H. K.; Werstiuk, N. H.; Bain, A. D.; McGlinchey, M. J. *Inorg. Chim. Acta* **1996**, *251*, 355−364. (c) Rigby, S. S.; Girard, L.; Bain, A. D.; McGlinchey, M. J. *Organometallics* **1995**, *14*, 3798−3801. (d) Chen, Y.-X.; Rausch, M. D.; Chien, J. C. W. *Organometallics* **1993**, *12*, 4607−4612. For problems in pK_a value determinations, caused by 1,5-sigmatropic shifts of silyl groups, see: (e) Bordwell, F. G.; Satish, A. V. J. *Am. Chem. Soc.* **1992**, *114*, 10173−10176. (f) Zhang, S.; Zhang, X.-M.; Bordwell, F. G. *J. Am. Chem. Soc.* **1995**, *117*, 602−606.

(71) Interestingly, the silylated indenyl compounds **8b** and **9b** show the same diastereotopic signal pattern (two doublets) for the two silylmethyl groups as the *ansa*-metallocene amide complexes described above. The signals of the Si−H moieties are shaped differently, additionally emphasizing the Ln···HSi coupling in the rare earth metallocene complexes.

(72) d$_\pi$−p$_\pi$ interactions for silylamines have been discussed controversely, see: Ebsworth, E. A. V. *Volatile Silicon Compounds*; Pergamon Press: Oxford, 1963.

(73) This could be independently proven by transsilylamination reactions of $NaN(SiMe_3)_2$ with bis(dimethylsilyl)amine: Eppinger, J.; Herdtweck, E.; Anwander, R. *Polyhedron* **1998**, *17*, 1195−1201.

Table 4. pK_a Values According to the Modified Method of Fraser

run	acid$_1$	ref. acid$_2$ (pK_2)	K_{eq}	$-\log K$	pK_1	lit. data
1	$HN(SiHMe_2)_2$	$HN(SiMe_3)_2$ (25.8)[a]	1.1×10^{-3}	3.0	22.8	
2	fluorene	$HN(SiMe_3)_2$ (25.8)[a]	0.020	1.7	24.2	24.4[a]/22.6[b]
3	fluorene	$HN(SiHMe_2)_2$ (22.8)	16	−1.2	24.0	24.4[a]/22.6[b]
4	indene	$HN(SiHMe_2)_2$ (22.8)	0.080	1.1	21.7	20.1[b]
5	fluorene	indene (21.7)	200	−2.3	24.0	24.4[a]/22.6[b]
6	$SiHMe_2$-Fluo (**10a**)	indene (21.7)	25	−1.4	23.1	21.7[b,c]
7	3-($SiHMe_2$)-Ind (**8a**)	indene (21.7)	0.032	1.5	20.2	
8	2-Me-Ind	indene (21.7)	30	−1.5	23.1	
9	3-($SiHMe_2$)-2-Me-Ind (**9a**)	indene (21.7)	0.050	0.3	21.4	

[a] Reference 65b. [b] In DMSO, refs 70e,f. [c] Trimethylsilyl derivative in DMSO.

This effect is less pronounced for the ligand 9-($SiMe_2$)fluorene ($\Delta pK_a = 0.9$). As expected, a methyl group in the 2-position increases the basicity of the indene molecule by 1.5 units.

These results show that the low yields isolated for the bis(indenyl) complexes *rac*-**13a** and **14b** are mainly due to sterically disfavored exchange reactions (kinetic control). In contrast, the synthesis of the silyl-linked bis(fluorenyl) complexes is additionally hampered by the low pK_a value of the bis(fluorene) precursors. Hence, an efficient preparation of fluorenyl-derived lanthanidocenes will require alternative amide precursors. For comparison, the pK_a criterion is of minor importance in related zirconocene chemistry,[19] where amine elimination reactions are routinely accomplished by utilizing more basic dialkylamide ligands (e.g, pK_a($HNiPr_2$) = 36.0).[66a]

Conclusion

A specialized silylamine elimination reaction gives access to a wide range of achiral and C_2-symmetric metallocene complexes of the rare earth elements, including the first Brintzinger-type lanthanide complexes. Utilization of tailor-made synthetic precursors such as $Ln[N(SiHMe_2)_2]_3(THF)_x$ seems to be the proper strategy to achieve exchange reactions with bulky, chelating molecules such as linked and substituted indene derivatives. The commercially available, sterically more encumbered standard systems $Ln[N(SiMe_3)_2]_3$, however, do not undergo these exchange reactions. Not only does the SiH moiety of the $[N(SiHMe_2)_2]$ ligands constitute an excellent spectroscopic probe to study these ligand-exchange reactions, but the steric and electronic peculiarities of the chelating ancillary ligands also imply a remarkable bis(dimethylsilyl)amide bonding. This bonding features a two-fold, strong Si−H metal coordination which is rigid in solution within a temperature range from −90 to 130 °C. This novel β-SiH diagostic interaction forces unprecedented large Si−N−Si angles and elongated Si−H bond distances, as revealed by spectroscopic and structural investigations. Such interactions resemble the early step of the oxidative addition of an Si−H bond to a metal center. Close M···SiH interactions (M = rare earth metal cation) are assumed mechanistic intermediates, e.g., in the dehydrogenative polymerization of hydrosilanes by lanthanidocene complexes.[74] The kinetic and thermodynamic limitations of this specialized silylamine elimination reaction could be rationalized on the basis of steric considerations and pK_a value determinations. To widen the scope of this synthetic route, i.e., better to cope with the prevailing synthetic limitations, we are currently evaluating additional tailor-made lanthanide amide precursors. Preliminary catalytic examinations clearly indicate an intriguing potential of this new generation of lanthanidocene complexes in both fine chemical and polymer synthesis.[75]

(74) (a) Forsyth, C. M.; Nolan, S. P.; Marks, T. J. *Organometallics* **1991**, *10*, 2543−2545. (b) Sakakura, T.; Lautenschlager, H.-J.; Nakajima, M.; Tanaka, M. *Chem. Lett.* **1991**, 913−916.

Experimental Section

General Considerations. All air- and moisture-sensitive compounds were manipulated with the rigorous exclusion of oxygen and moisture in flame-dried (180 °C) Schlenk-type glassware using the standard high-vacuum technique or an argon-filled glovebox (MBraun) with O_2/H_2O < 1 ppm. The solvents were predried, distilled from Na/K alloy, and stored in a glovebox. Deuterated solvents were obtained from Deutero GmbH and degassed and dried over Na/K alloy.

Fluorene and 2-methylindene were purchased from Aldrich and used as received. Indene (90%, Aldrich) was distilled and stored under nitrogen at −35 °C. Dimethyldichlorosilane and dimethylchlorosilane (Aldrich) were freshly distilled from potassium carbonate prior to use. Bis(2,3,4,5-tetramethylcyclopenta-2,4-dien-1-yl)dimethylsilane ($Me_2Si(Cp''H)_2$, **1**)[24] and bis(fluoren-9-yl)dimethylsilane ($Me_2Si(FluoH)_2$, **6**)[26] were synthesized according to published procedures by reacting the corresponding lithiated hydrocarbons with dimethyldichlorosilane. Lithiation of the hydrocarbons indene, 2-methylindene, fluorene, and the silylamines 1,1,1,3,3,3,-hexamethyldisilazane and 1,1,3,3,-tetramethyldisilazane was carried out by adding *n*-butyllithium (1.6 M solution in hexane) to an *n*-hexane solution at −78 °C. Tetrahydrofurantris[bis(dimethylsilyl)amido]scandium(III) (**7a**) and the *trans*-bis(tetrahydrofuran)tris[bis(dimethylsilyl)amido]lanthanoid(III) precursors **7b**−**e** were prepared as described recently.[15] $Y[N(SiMe_3)_2]_3$ was prepared from $YCl_3(THF)_3$ and $K[N(SiMe_3)_2]$ and sublimed prior to use. 2,2-Bis(inden-1-yl)propane ($Me_2C(IndH)_2$, **2**) and bis(2-methyl-4-phenylinden-1-yl)-dimethylsilane ($Me_2Si(2\text{-}Me\text{-}4\text{-}Ph\text{-}IndH)_2$, **4**) were donated by Hoechst AG. Bis(2-methylinden-1-yl)dimethylsilane ($Me_2Si(2\text{-}Me\text{-}IndH)_2$, **3**) and bis(2-methyl-4,5-benzoinden-1-yl)dimethylsilane ($Me_2Si(2\text{-}Me\text{-}Benz\text{-}IndH)_2$, **5**) were donated by Peroxid GmbH (Laporte). For the preparation of these ligands see ref 25.

NMR spectra were recorded either on a Bruker DPX-400 (FT, 400 MHz ^1H; 100 MHz ^{13}C) or on a JEOL JNM-GX-400 (FT, 400 MHz ^1H; 100 MHz ^{13}C; 79.5 MHz ^{29}Si) spectrometer. ^1H and ^{13}C shifts are referenced to internal solvent resonances and reported relative to TMS. The NOE experiment was recorded on the Bruker spectrometer. ^{89}Y NMR experiments were performed on the JEOL spectrometer, which was equipped with a broad-band 10-mm probe (19.48 MHz ^{89}Y, 3.0 M YCl_3 in D_2O as a standard, sample concentration 0.26 M in a 6:1 mixture of toluene/C_6D_6; acquisition parameters, pulse width 10 ms, pulse delay 20 s, 3000 scans). IR spectra were recorded on a Perkin-Elmer 1650-FTIR spectrometer as Nujol mulls. Mass spectra (CI; ionization agent, isobutene) were obtained on a Finnigan MAT-90 spectrometer. Elemental analyses were performed in the microanalytical laboratory of the institute.

pK_a Value Measurements. The pK_a values of tetramethyldisilazane, inden-1-yldimethylsilane, (2-methylinden-1-yl)dimethylsilane, and flouren-1-yldimethylsilane were determined by a slight modification of the procedure described by Fraser et al.[65] In a glovebox, the lithiated reference acid (lithium bis(trimethylsilyl)amide, lithium bis(dimethylsilyl)amide, indenyllithium, fluorenyllithium) was mixed with an equimolar amount of the protonated acid and 0.33 equiv of hexamethylbenzene as an internal standard. The mixture was cooled to −35 °C and dissolved in a 20:1 mixture of C_6D_6 and THF-d_8 to give a 0.1 M solution. After 30 min the solution was transferred into a 10-mm

(75) Anwander R.; Görlitzer, H. W.; Gerstberger, G.; Eppinger, J., unpublished results.

sealable NMR tube, allowed to warm to ambient temperature, and placed in the Bruker spectrometer operating at 25 °C. ^{13}C NMR spectra were accumulated immediately using a small pulse angle (30°) and a 2-s repetition rate (a repetition rate of 4 s did not affect the integral ratios). Influences such as differential NOEs were eliminated by using an empirically derived correction factor. This factor was determined by measuring the integrals of the protonated and lithiated compounds relative to a certain amount of hexamethylbenzene as an internal standard. In accordance with Fraser et al.,[65] we estimated the accuracy of *K*, derived from the equilibrium concentrations of all species present in the solution, to be ±30%, i.e., an uncertainty of ΔpK_a of ±0.2 pK_a unit or less. The ^{13}C NMR shifts were (400 MHz, 25 °C) as follow: HN(SiMe$_3$)$_2$, δ 4.19; LiN(SiMe$_3$)$_2$, δ 3.17; HN(SiHMe$_2$)$_2$, δ 1.54; LiN(SiHMe$_2$)$_2$, δ 2.62; IndH, δ 144.7, 143.5, 133.8, 132.1, 126.1, 124.5, 123.6, 120.9, 39.1; Li(Ind), δ 128.4, 120.5, 115.7, 115.4, 91.9; 2-Me-IndH, δ 146.7, 145.4, 145.0, 126.0, 125.5, 125.3, 122.8, 120.3, 46.8, 16.73; Li(2-Me-Ind), δ 128.2, 125.7, 119.4, 115.5, 92.2, 14.83; FluoH, δ 142.2, 141.0, 127.1, 125.8, 124.2, 120.4, 40.13; Li(Fluo), δ 136.5, 121.8, 120.1, 119.3, 116.6, 109.5, 80.4; C$_6$Me$_6$, δ 131.71, 16.86.

General Procedure for the Silylation of Indenyl and Fluorenyl Systems. Over a period of 30 min, 1.0 equiv of *n*-butyllithium (1.6 M solution in hexane) was added dropwise to a solution of the corresponding aromatic hydrocarbon in THF (5 mL/mmol of the reactants) at − 78 °C. The cold reaction mixture was stirred for 2 h. Then 1.1 equiv of dimethylchlorosilane in THF (5 mL/mmol) was added dropwise at −78 °C, and the mixture was stirred at this temperature for 1 h. The reaction mixture was allowed to warm to ambient temperature and stirred for another 12 h before the solvent was removed in vacuo. The residue was suspended in *n*-hexane (10 mL/mmol of the desired product) and refluxed for 30 min. After the hexane suspension was cooled to ambient temperature, LiCl was filtered off, and the residue was washed a second time with the same amount of *n*-hexane. The pure product was obtained by removing the solvent from the combined organic phases.

Dimethylsilylindene (8a). Following the procedure described above, indene (1.564 g, 18.17 mmol), *n*-butyllithium (1.60 M in hexane, 11.4 mL, 18.2 mmol), and dimethylchlorosilane (1.89 g, 20.0 mmol) yielded **8a** (2.587 g, 14.84 mmol, 82%) as a pale yellow oil. IR (neat, cm^{-1}): 3115 w, 3065 m, 3052 m, 3015 w, 2959 m, 2901 w, 2120 vs (ν(Si−H)), 1938 w, 1900 w, 1833 w, 1789 w, 1722 w, 1626 w, 1605 w, 1580 w, 1536 w, 1459 m, 1450 s, 1422 w, 1360 w, 1311 w, 1250 s, 1220 m, 1190 m, 1112 w, 1029 vs, 980 m, 934 m, 886 vs, 860 s, 837 s, 801 s, 766 vs, 728 m, 716 s, 675 m, 644 m, 632 m, 600 w, 564 m, 540 m, 455 s, 420 w. ^{1}H NMR (400 MHz, C$_6$D$_6$, 25 °C): (a) major isomer (3-dimethylsilylindene, 94 mol %): δ 7.42 (dd, ^3J(H,H) = 7.7 Hz, ^4J(H,H) = 0.9 Hz, 1 H, indenyl-H), 7.40 (dd, ^3J(H,H) = 7.7 Hz, ^4J(H,H) = 1.0 Hz, 1 H, indenyl-H), 7.21 ("t", ^3J(H,H) = 7.5 Hz, 1 H, indenyl-H), 7.15 ("t", ^3J(H,H) = 7.3 Hz, 1 H, indenyl-H), 6.83 (dd, ^3J(H,H) = 5.2 Hz, ^4J(H,H) = 0.7 Hz, 1 H, indenyl-H), 6.43 (dd, ^3J(H,H) = 5.1 Hz, ^3J(H,H) = 1.9 Hz, 1 H, indenyl-H), 4.26 (dsept, ^1J(Si,H) = 189 Hz, ^3J(H,H) = 3.4 Hz, ^3J(H,H) = 1.0 Hz, 1 H, SiH), 3.48 (d, ^3J(H,H) = 1.6 Hz, 1 H, indenyl-H), −0.17 (d, ^3J(H,H) = 3.6 Hz, 6 H, HSi(CH_3)$_2$(I)), −0.27 (d, ^3J(H,H) = 3.6 Hz, 6 H, HSi(CH_3)$_2$(II)); (b) minor isomer (1-dimethylsilylindene, 6 mol %): δ 7.51 (dd, 1 H, indenyl-H), 7.28 ("t", 1 H, indenyl-H), 7.10 ("t", 1 H, indenyl-H), 6.72 (dd, 1 H, indenyl-H), 6.23 (dd, 1 H, indenyl-H), 4.40 (sept, 1 H, SiH), 3.03 (t, 1 H, indenyl-H), 0.13 (d, 6 H, HSi(CH_3)$_2$(I)), −0.10 (d, 6 H, HSi(CH_3)$_2$(II)). ^{13}C{^{1}H} NMR (100.5 MHz, C$_6$D$_6$, 25 °C): δ 145.3, 144.5, 135.0, 129.8, 125.5, 124.4, 123.0, 121.5, (s, indenyl-C), 43.80 (s, α-C), −5.25 (s, HSi(*C*H$_3$)$_2$(I)), −6.46 (s, HSi(*C*H$_3$)$_2$(II)). MS (EI): *m*/*z* (relative intensity) 174 (21) [M$^+$], 159 (34) [M$^+$ − CH$_3$)], 115 (17) [M$^+$ − SiHMe$_2$], 59 (100) [SiHMe$_2^+$]. Anal. Calcd for C$_{11}$H$_{14}$Si: C, 75.71; H, 8.09. Found: C, 76.26; H, 8.20.

3-Dimethylsilyl-2-methylindene (9a). Following the procedure described above, 2-methylindene (1.175 g, 9.03 mmol), *n*-butyllithium (1.60 M in hexane, 5.6 mL, 9.0 mmol), and dimethylchlorosilane (0.946 g, 10.0 mmol) yielded **9a** (1.460 mg, 7.75 mmol, 86%) as a pale yellow oil. IR (neat, cm^{-1}): 3063 s, 3052 s, 3013 m, 2960 s, 2908 s, 2855 w, 2734 w, 2120 vs (ν(Si−H)), 1932 w, 1896 w, 1859 w, 1794 w, 1680 w, 1605 w, 1593 m, 1567 w, 1457 s, 1447 s, 1379 w, 1300 m, 1250 s, 1220 m, 1194 m, 1153 w, 1120 w, 1100 w, 1051 s, 1012 s, 930 m, 889 vs, 836 vs, 801 s, 782 s, 750 vs, 730 m, 714 s, 683 w, 647 s, 630 m, 602 m, 566 m, 477 m, 455 s, 424 w. ^{1}H NMR (400 MHz, C$_6$D$_6$, 25 °C): δ 7.34 (d, ^3J(H,H) = 7.7 Hz, 1 H, indenyl-H), 7.32 (d, ^3J(H,H) = 7.3 Hz, 1 H, indenyl-H), 7.21 ("t", ^3J(H,H) = 7.5 Hz, 1 H, indenyl-H), 7.11 ("dt", ^3J(H,H) = 7.3 Hz, 1 H, ^4J(H,H) = 0.7 Hz, indenyl-H), 6.46 (s, 1 H, indenyl-H), 4.25 (dsept, ^1J(Si,H) = 190 Hz, ^3J(H,H) = 3.6 Hz, ^3J(H,H) = 1.0 Hz, 1 H, SiH), 3.14 (d, ^3J(H,H) = 1.0 Hz, 1 H, indenyl-H), 2.00 (s, 3 H, indenyl-C*H*$_3$), −0.08 (d, ^3J(H,H) = 3.6 Hz, 6 H, HSi(C*H*$_3$)$_2$(I)), −0.35 (d, ^3J(H,H) = 3.6 Hz, 6 H, HSi(C*H*$_3$)$_2$(II)). ^{13}C{^{1}H} NMR (100.5 MHz, C$_6$D$_6$, 25 °C): δ 146.7, 145.4, 145.0, 126.0, 125.5, 123.3, 122.8, 120.3, (s, indenyl-C), 46.78 (s, α-C), 16.73 (s, indenyl-*C*H$_3$), −6.03 (s, HSi(*C*H$_3$)$_2$(I)), −7.19 (s, HSi(*C*H$_3$)$_2$(II)). MS (EI): *m*/*z* (relative intensity) 188 (33) [M$^+$], 173 (20) [M$^+$ − CH$_3$)], 129 (45) [M$^+$ − SiH(CH$_3$)$_2$], 59 (100) [SiH(CH$_3$)$_2^+$]. Anal. Calcd for C$_{12}$H$_{16}$Si: C, 76.52; H, 8.56. Found: C, 75.16; H, 8.84.

9-(Dimethylsilyl)fluorene (10a). Following the procedure described above, fluorene (1.662 g, 10.00 mmol), *n*-butyllithium (1.60 M in hexane, 6.25 mL, 10.0 mmol), and dimethylchlorosilane (1.04 g, 11.0 mmol) yielded **10a** (1.963 g, 8.75 mmol, 87%) as a white powder. IR (Nujol, cm^{-1}): 3065 w, 2926 vs, 2853 vs, 2724 s, 2122 s (ν(Si−H)), 1938 w, 1901 w, 1795 w, 1615 w, 1576 w, 1460 s, 1402 w, 1377 s, 1310 w, 1298 w, 1250 m, 1186 m, 1098 w, 1055 m, 1028 w, 1005 w, 973 w, 952 w, 933 w, 885 s, 860 w, 838 w, 795 w, 738 vs, 694 w, 646 w, 621 m, 486 w, 426 w, 411 m. ^{1}H NMR (400 MHz, C$_6$D$_6$, 25 °C): δ 7.74 (dd, ^3J(H,H) = 6.6 Hz, ^4J(H,H) = 1.5 Hz, 2 H, fluorenyl-H), 7.42 (dd, ^3J(H,H) = 7.0 Hz, ^4J(H,H) = 1.3 Hz, 2 H, fluorenyl-H), 7.26 ("t", ^3J(H,H) = 7.0 Hz, 2 H, fluorenyl-H), 7.22 ("dt", ^3J(H,H) = 6.5 Hz, ^4J(H,H) = 1.5 Hz, 2 H, fluorenyl-H), 4.26 (dsept, ^1J(Si,H) = 184 Hz, ^3J(H,H) = 3.7 Hz, 1 H, SiH), 3.48 (s, 1 H, fluorenyl-H), −0.28 (d, ^3J(H,H) = 3.7 Hz, 12 H, HSi(C*H*$_3$)$_2$). ^{13}C{^{1}H} NMR (100.5 MHz, C$_6$D$_6$, 25 °C): δ 145.5, 143.5, 127.0, 126.6, 125.2, 120.1 (s, fluorenyl-C), 36.91 (s, α-C), −6.42 (s, HSi(*C*H$_3$)$_2$). MS (EI): *m*/*z* (relative intensity) 224 (41) [M$^+$], 209 (17) [M$^+$ − CH$_3$)], 165 (43) [M$^+$ − SiHMe$_2$], 59 (100) [SiHMe$_2^+$]. Anal. Calcd for C$_{15}$H$_{16}$Si: C, 80.29; H, 7.19. Found: C, 81.40; H, 7.07.

General Procedure for the Lithiation of Silylated Indenyl and Fluorenyl Systems. Over a period of 10 min, 1.0 equiv of *n*-butyllithium (1.6 M solution in hexane) was added dropwise to a solution of the corresponding silylated aromatic hydrocarbon in *n*-hexane (5 mL/mmol of the reactants) at − 78 °C. After being stirred for 2 h at low temperature, the reaction mixture was stirred for an additional 2 h at ambient temperature before the insoluble product was separated via filtration. The residue was washed with cold *n*-hexane (2 mL/mmol desired product) and dried in vacuo, yielding the pure product.

3-(Dimethylsilyl)indene Lithium (8b). Following the procedure described above, 3-dimethylsilylindene **(8a)** (1.451 g, 8.32 mmol) and *n*-butyllithium (1.60 M in hexane, 5.2 mL, 8.3 mmol) yielded **8b** (0.934 g, 5.18 mmol, 62%) as a white powder. IR (Nujol, cm^{-1}): 2924 vs, 2734 w, 2094 m (ν(Si−H)), 1463 vs, 1377 s, 1318 m, 1288 w, 1257 m, 1212 m, 1155 m, 1141 w, 1033 m, 991 w, 970 m, 941 w, 894 m, 868 m, 834 m, 753 sh, 722 m, 668 m, 630 w, 534 sh, 467 brm. ^{1}H NMR (400 MHz, C$_6$D$_6$, 25 °C): δ 7.89 (m, 2 H, indenyl-H), 7.40 (dd, ^3J(H,H) = 7.7 Hz, ^4J(H,H) = 1.0 Hz, 1 H, indenyl-H), 7.11−7.05 (m, 3 H, indenyl-H), 6.49 (d, ^3J(H,H) = 3.5 Hz, 1 H, indenyl-H), 5.27 (sept, ^1J(Si,H) = 176 Hz, ^3J(H,H) = 3.6 Hz, 1 H, SiH), 0.62 (d, ^3J(H,H) = 3.9 Hz, 6 H, HSi(C*H*$_3$)$_2$(I)). ^{13}C{^{1}H} NMR (100.5 MHz, C$_6$D$_6$, 25 °C): δ 134.9, 132.4, 127.2, 125.5, 124.2, 121.4, 116.9, 116.7, 96.4 (s, indenyl-C), −1.08 (s, HSi(*C*H$_3$)$_2$). Anal. Calcd for C$_{11}$H$_{13}$LiSi: C, 73.30; H, 7.27. Found: C, 74.23; H, 6.84.

3-Dimethylsilyl-2-methylindene Lithium (9b). Following the procedure described above, 3-dimethylsilyl-2-methylindene (**9a**) (1.147 g, 6.12 mmol) and *n*-butyllithium (1.60 M in hexane, 3.8 mL, 6.1 mmol) yielded **9b** (0.842 g, 4.33 mmol, 71%) as a white powder. IR (neat, cm^{-1}): 2921 vs, 2723 w, 2083 s (ν(Si−H)), 1463 vs, 1411 w, 1377 s, 1350 m, 1336 m, 1267 m, 1244 m, 1203 w, 1153 w, 1120 w, 1052 m, 1000 w, 908 w, 881 s, 833 s, 801 s, 760 s, 734 s, 696 w, 669 w, 647 m, 483 brs. ^{1}H NMR (400 MHz, C$_6$D$_6$, 25 °C): δ 7.95 (d, ^3J(H,H) = 8.4 Hz, 1 H, indenyl-H), 7.33 (d, ^3J(H,H) = 7.5 Hz, 1 H, indenyl-H), 7.06−7.01 (m, 2 H, indenyl-H), 6.24 (s, 1 H, indenyl-H), 5.31 (sept, ^1J(Si,H) = 180 Hz, ^3J(H,H) = 3.9 Hz, 1 H, SiH), 2.66 (s, 3 H, indenyl-

CH_3), 0.62 (d, ^3J(H,H) = 4.0 Hz, 6 H, HSi(CH_3)$_2$(I)). ^{13}C{^{1}H} NMR (100.5 MHz, C_6D_6, 25 °C): δ 135.8, 135.7, 131.1, 120.6, 119.6, 119.5, 116.4, 115.6, 91.6, (s, indenyl-C), 17.28 (s, indenyl-CH_3), −0.36 (s, HSi(CH_3)$_2$). Anal. Calcd for $C_{12}H_{15}LiSi$: C, 74.19; H, 7.78. Found: C, 73.95; H, 7.37.

9-(Dimethylsilyl)fluorene Lithium (10b). Following the procedure described above, 9-(dimethylsilyl)fluorene (**10a**) (1.122 g, 5.00 mmol) and *n*-butyllithium (1.60 M in hexane, 3.1 mL, 5.0 mmol) yielded **10b** (0.671 mg, 2.92 mmol, 58.3%) as a white powder. IR (Nujol, cm^{-1}): 2923 vs, 2854 vs, 2724 w, 2085 s (ν(Si−H)), 1577 w, 1463 vs, 1377 s, 1321 s, 1266 w, 1212 m, 1200 w, 1151 w, 1096 w, 1067 m, 1043 w, 1008 w, 988 m, 926 w, 842 w, 821 w, 770 w, 751 m, 726 s, 688 w, 542 m, 494 w, 429 m. ^{1}H NMR (400 MHz, C_6D_6, 25 °C): δ 8.08 (d, ^3J(H,H) = 8.0 Hz, 2 H, fluorenyl-H), 7.76 (d, ^3J(H,H) = 7.9 Hz, 2 H, fluorenyl-H), 7.25 ("t", ^3J(H,H) = 8.0 Hz, 2 H, fluorenyl-H), 7.12 ("t", ^3J(H,H) = 7.6 Hz, 2 H, fluorenyl-H), 5.53 (sept, ^1J(Si,H) = 168 Hz, ^3J(H,H) = 3.8 Hz, 1 H, SiH), 0.71 (d, ^3J(H,H) = 3.9 Hz, 12 H, HSi(CH_3)$_2$). ^{13}C{^{1}H} NMR (100.5 MHz, C_6D_6, 25 °C): δ 142.3, 127.2, 121.7, 121.0, 119.1, 117.1, 111.5 (s, fluorenyl-C), −0.57 (s, HSi(CH_3)$_2$). Anal. Calcd for $C_{15}H_{15}LiSi$: C, 78.23; H, 6.56. Found: C, 77.37; H, 6.81.

General Procedure for the Preparation of *ansa*-Lanthanidocene Amides. In a glovebox, Ln[N(SiHMe$_2$)$_2$]$_3$(THF)$_x$ (**7a**−**e**) and the equimolar amount of ligand **1**−**6** were dissolved in toluene (20 mL/mmol silylamide), refluxed for the time mentioned below, and evaporated to dryness. For the bis(indene) or bis(fluorene) **2**−**6**, the residue was dissolved in mesitylene (20 mL/mmol silylamide) and refluxed a second time. After the solvent was removed in vacuo, the resulting powder was dissolved in toluene. The filtrated solution was cooled to −45 °C, upon which a microcrystalline precipitate formed. After the solvent was decanted, this precipitate was dissolved in hot *n*-hexane and cooled slowly to −45 °C, at which temperature pure **11b**,**c**−**16b** were obtained as single crystals. This procedure could be scaled up from 0.5 to 20 mmol.

[Bis(dimethylsilyl)amido][η^5:η^5-bis(2,3,4,5-tetramethylcyclopentadien-1-yl)dimethylsilyl]yttrium(III) (11b). Following the procedure described above, **7b** (630.1 mg, 1.000 mmol) and **1** (300.6 mg, 1.000 mmol) yielded **11b** (462.2 mg, 0.820 mmol, 82%) as colorless prisms (15 h of refluxing in toluene). IR (Nujol, cm^{-1}): 2922 vs, 2853 vs, 2724 m, 1789 brw (ν(Si−H)), 1463 vs, 1377 s, 1371 sh, 1312 m, 1244 m, 1154 w, 1086 w, 1020 m, 972 w, 905 brm, 900 w, 836 w, 811 w, 761 w, 722 m, 676 m, 462 w. ^{1}H NMR (400 MHz, C_6D_6, 25 °C): δ 4.00 (dsept, ^1J(Y,H) = 2.9 Hz, ^1J(Si,H) = 147 Hz, ^3J(H,H) = 2.70 Hz, 2 H, SiH), 2.06 (s, 12 H, Cp(CH_3)(I)), 1.95 (s, 12 H, Cp(CH_3)(II)), 0.97 (s, 6 H, Cp″$_2$Si(CH_3)$_2$), 0.24 (d, ^3J(H,H) = 2.5 Hz, 12 H, HSi(CH_3)$_2$). ^{13}C{^{1}H} NMR (100.5 MHz, C_6D_6, 25 °C): δ 127.3 (s, C_{Cp}(I)), 122.8 (s, C_{Cp}(II)), 108.7 (s, SiC_{Cp}), 14.5 (s, Cp(*C*H$_3$)(I)), 12.0 (s, Cp(*C*H$_3$)(II)), 4.33 (s, Cp″$_2$Si(*C*H$_3$)$_2$), 3.55 (s, HSi(CH$_3$)$_2$). ^{29}Si{^{1}H} NMR (79.5 MHz, C_6D_6, 25 °C): δ −19.87 (s, NSi), −32.45 (brs, Si_{bridge}). MS (CI): *m*/*z* (relative intensity) 519 (14) [M$^+$], 447 (8) [M$^+$ − N(SiHMe$_2$)], 389 (3) [M$^+$ − N(SiHMe$_2$)$_2$ + 2H], 331 (46) [Y(Cp″)$^+$], 316 (100) [SiMe$_2$(Cp″)CH$_4^+$], 301 (16) [SiMe$_2$(Cp″)H$^+$], 179 (7) [SiMe$_2$(Cp″)$^+$], 118 (2) [N(SiHMe$_2$)(SiHMe)$^+$]. Anal. Calcd for $C_{24}H_{44}NSi_3Y$: C, 55.46; H, 8.53; N, 2.69. Found: C, 54.24; H, 8.89; N, 2.37.

[Bis(dimethylsilyl)amido][η^5:η^5-bis(2,3,4,5-tetramethylcyclopentadien-1-yl)dimethylsilyl]lanthanum(III) (11c). Following the procedure described above, **7c** (340.1 mg, 0.500 mmol) and **1** (150.3 mg, 0.500 mmol) yielded **11c** (273.5 mg 0.480 mmol, 96%) as colorless prisms (15 h of refluxing in toluene). IR (Nujol, cm^{-1}): 2922 vs, 2853 vs, 2723 m, 1845 brw (ν(Si−H)), 1462 vs, 1454 vs, 1377 s, 1250 m, 1161 w, 1100 w, 1092 w, 1015 w, 974 w, 928 m, 900 w, 881 w, 834 w, 801 w, 723 m, 663 w. ^{1}H NMR (400 MHz, C_6D_6, 25 °C): δ 4.18 (m, ^1J(Si,H) = 150 Hz, 2 H, SiH), 2.18 (s, 12 H, Cp(CH_3)(I)), 1.95 (s, 12 H, Cp(CH_3)(II)), 0.95 (s, 6 H, Cp″$_2$Si(CH_3)$_2$), 0.19 (d, ^3J(H,H) = 2.5 Hz, 12 H, HSi(CH_3)$_2$); ^{13}C{^{1}H} NMR (100.5 MHz, C_6D_6, 25 °C): δ 127.3 (s, C_{Cp}(I)), 126.1 (s, C_{Cp}(II)), 110.5 (s, SiC_{Cp}), 14.5 (s, Cp-(*C*H$_3$)(I)), 11.3 (s, Cp(*C*H$_3$)(II)), 4.50 (s, Cp″$_2$Si(*C*H$_3$)$_2$), 2.23 (s, HSi-(CH$_3$)$_2$). ^{29}Si{^{1}H} NMR (79.5 MHz, C_6D_6, 25 °C): δ −17.31 (s, NSi), −30.41 (brs, Si_{bridge}). MS (CI): *m*/*z* (relative intensity) 569 (85) [M$^+$], 554 (15) [M$^+$ − CH$_3$], 437 (100) [M$^+$ − N(SiHMe$_2$)$_2$], 421 (12) [M$^+$ − N(SiHMe$_2$)$_2$ − CH$_3$], 179 (7) [SiMe$_2$(Cp″)$^+$], 118 (2) [N(SiHMe$_2$)-(SiHMe)$^+$]. Anal. Calcd for $C_{24}H_{44}LaNSi_3$: C, 50.59; H, 7.78; N, 2.46. Found: C, 50.47; H, 8.14; N, 2.28.

***rac*-[Bis(dimethylsilyl)amido][η^5:η^5-bis-2,2-(inden-1-yl)propyl]-yttrium(III) (*rac*-12b).** Following the procedure described above, **7b** (630.1 mg, 1.000 mmol) and **2** (274.0 mg, 1.000 mmol) yielded *rac*-**12b** (69.8 mg, 0.142 mmol, 14%) as yellow prisms (15 h of refluxing in toluene and 5 h of refluxing in mesitylene). IR (Nujol, cm^{-1}): 2922 vs, 2853 vs, 2723 m, 1821 w (ν(Si−H)), 1461 vs, 1377 s, 1306 w, 1246 m, 1216 w, 1204 w, 1153 w, 1044 w, 1003 w, 915 m, 896 m, 842 m, 804 w, 766 m, 749 s, 743 m, 721 m, 685 w; 672 w, 611 w, 468 w, 454 m, 427 w. ^{1}H NMR (400 MHz, C_6D_6, 75 °C): δ 7.74 (d, ^3J(H,H) = 8.6 Hz, 2 H, H4), 7.39 (d, ^3J(H,H) = 8.0 Hz, 2 H, H6), 6.91 (dd, 2× ^3J(H,H) = 7.5 Hz, 2 H, H5), 6.73 (dd, 2× ^3J(H,H) = 7.3 Hz, 2 H, H7), 6.62 (d, ^3J(H,H) = 3.0 Hz, 2 H, H2), 6.19 (d, ^3J(H,H) = 3.1 Hz, 2 H, H3), 3.56 (dsept, ^1J(Si,H) = 152 Hz, ^3J(H,H) = 2.8 Hz, 2 H, SiH), 2.14 (s, 6 H, C(CH_3)$_2$), 0.11 (d, ^3J(H,H) = 2.7 Hz, 6 H, HSiCH_3-(I)), 0.07 (d, ^3J(H,H) = 2.7 Hz, 6 H, HSiCH_3(II)). ^{13}C{^{1}H} NMR (100.5 MHz, C_6D_6, 60 °C): δ 126.2/125.8/123.7/123.0/121.6/118.9/114.6/109.1/101.7 (s, indenyl-C), 40.5 (s, bridge-C), 28.9 (s, C(CH_3)$_2$), 2.59 (s, HSi(CH$_3$)$_2$(I)), 2.07 (s, HSi(CH$_3$)$_2$(II)). MS (CI): *m*/*z* (relative intensity) = 851 (6) [M$^+$ + Y(Me$_2$CInd$_2$)], 845 (3) [M$^+$ + Y(N(SiHMe$_2$)$_2$)$_2$], 491 (100) [M$^+$], 476 (12) [M$^+$ − CH$_3$], 359 (14) [M$^+$ − N(SiHMe$_2$)$_2$], 272 (2) [Me$_2$CInd$_2^+$], 247 (4) [M$^+$ − N(SiHMe$_2$)$_2$ − Ind + 2H], 132 (4) [N(SiHMe$_2$)$_2^+$], 118 (7) [N(SiHMe$_2$)(SiHMe)$^+$]. Anal. Calcd for $C_{25}H_{32}NSi_2Y$: C, 61.08; H, 6.56; N, 2.85. Found: C, 59.18; H, 6.70; N, 2.48.

***rac*-[Bis(dimethylsilyl)amido][η^5:η^5-bis(2-methylinden-1-yl)-dimethylsilyl]scandium(III) (*rac*-13a).** Following the procedure described above, **7a** (1028.1 mg, 2.000 mmol) and **3** (633.0 mg, 2.000 mmol) yielded *rac*-**13a** (201.4 mg, 0.410 mmol, 20%) as lemon yellow prisms (24 h of refluxing in toluene and 12 h of refluxing in mesitylene). IR (Nujol, cm^{-1}): 2924 vs, 2953 vs, 2724 w, 2012 m, 1793 brw (ν-(Si−H)), 1460 vs, 1377 vs, 1346 w, 1304 w, 1272 w, 1245 s, 1152 w, 1072 m, 1038 brm, 1000 m, 898 s, 834 s, 806 s, 802 s, 764 m, 744 m, 721 w, 691 m, 654 w, 611 w, 566 w, 484 w, 455 s. ^{1}H NMR (400 MHz, C_6D_6, 25 °C): δ 7.78 (d, ^3J(H,H) = 8.5 Hz, 2 H, H7), 7.49 (d, ^3J(H,H) = 7.5 Hz, 2 H, H4), 6.85 (dd, 2× ^3J(H,H) = 7.5 Hz, 2 H, H6), 6.80 (dd, 2× ^3J(H,H) = 7.5 Hz, 2 H, H5), 6.23 (s, 2 H, H3), 2.96 (m, ^1J(Si,H) = 155 Hz, ^3J(H,H) = 2.5 Hz, 2 H, SiH), 2.27 (s, 6 H, CH_3-indenyl), 1.12 (s, 6 H, Si(CH$_3$)$_2$), 0.11 (d, ^3J(H,H) = 2.5 Hz, 6 H, HSiCH_3(I)), 0.060 (d, ^3J(H,H) = 2.5 Hz, 6 H, HSiCH_3(II)). ^{13}C{^{1}H} NMR (100.5 MHz, C_6D_6, 25 °C): δ 136.9/132.8/131.8/125.0/124.8/122.9/122.8/113.2 (s, C2−C9), 100.8 (s, C1), 18.8 (s, *C*H$_3$-indenyl), 3.45 (s, HSi*C*H$_3$), 3.07 (s, Si*C*H$_3$). MS (CI): *m*/*z* (relative intensity) 491 (16) [M$^+$], 476 (10) [M$^+$ − CH$_3$], 432 (12) [M$^+$ − SiHMe$_2$], 359 (10) [M$^+$ − N(SiHMe$_2$)$_2$], 316 (30) [SiMe$_2$(Me-Ind)$_2$H$^+$], 301 (14) [SiMe$_2$(Me-Ind)$_2$H$^+$ − CH$_3$], 187 (100) [SiMe$_2$(Me-Ind)H$^+$], 159 (6) [Si(Me-Ind)H$_2^+$], 132 (2) [N(SiHMe$_2$)$_2^+$]. Anal. Calcd for $C_{26}H_{36}NSi_3Sc$: C, 63.50; H, 7.38; N, 2.85. Found: C, 62.48; H, 7.33; N, 2.53.

***rac*-[Bis(dimethylsilyl)amido][η^5:η^5-bis(2-methylinden-1-yl)-dimethylsilyl]yttrium(III) (*rac*-13b).** Following the procedure described above, **7b** (630.1 mg, 1.000 mmol) and **3** (316.5 mg, 1.000 mmol) yielded *rac*-**13b** (278.3 mg, 0.520 mmol, 52%) as lemon yellow prisms (15 h of refluxing in toluene and 3 h of refluxing in mesitylene). IR (Nujol, cm^{-1}): 2922 vs, 2853 vs, 2723 m, 1804 brw (ν(Si−H)), 1464 vs, 1410 w, 1379 s, 1344 m, 1333 m, 1279 m, 1246 s, 1150 m, 1037 m, 1000 m, 902 m, 876 s, 833 s, 807 s, 781 s, 765 s, 748 s, 690 m, 656 w, 644 m, 611 w, 571 w, 484 w, 460m, 449 s, 429 m. ^{1}H NMR (400 MHz, C_6D_6, 25 °C): δ 7.87 (d, ^3J(H,H) = 8.5 Hz, 2 H, H7), 7.38 (d, ^3J(H,H) = 7.8 Hz, 2 H, H4), 6.91 (dd, 2× ^3J(H,H) = 7.6 Hz, 2 H, H6), 6.84 (dd, 2× ^3J(H,H) = 8.5 Hz, 2 H, H5), 6.15 (s, 2 H, H3), 2.98 (dsept, ^1J(Y,H) = 4.6 Hz, ^1J(Si,H) = 142 Hz, ^3J(H,H) = 2.4 Hz, 2 H, SiH), 2.39 (s, 6 H, CH_3-indenyl), 1.10 (s, 6 H, Si(CH$_3$)$_2$), 0.067 (d, ^3J(H,H) = 2.4 Hz, 6 H, HSiCH_3(I)), 0.034 (d, ^3J(H,H) = 2.4 Hz, 6 H, HSiCH_3(II)). ^{13}C{^{1}H} NMR (100.5 MHz, C_6D_6, 25 °C): δ 138.0/131.3/131.0/123.4/123.3/122.1/121.9/108.2 (s, C2−C9), 99.3 (s, C1), 18.0 (s, *C*H$_3$-indenyl), 3.15 (s, SiCH$_3$), 2.66 (s, HSi*C*H$_3$(I)), 2.64 (s, HSi*C*H$_3$-(II)). MS (CI): *m*/*z* (relative intensity) 535 (6) [M$^+$], 316 (32) [SiMe$_2$-(Me-Ind)$_2$H$^+$], 187 (100) [SiMe$_2$(Me-Ind)H$^+$], 132 (7) [N(SiHMe$_2$)$_2^+$]. Anal. Calcd for $C_{26}H_{36}NSi_3Y$: C, 58.29; H, 6.77; N, 2.61. Found: C, 56.32; H, 6.80; N, 2.34.

***rac*-[Bis(dimethylsilyl)amido][η^5:η^5-bis(2-methylinden-1-yl)-dimethylsilyl]lanthanum(III) (*rac*-13c).** Following the procedure described above, **7c** (328.8 mg, 0.483 mmol) and **3** (152.9 mg, 0.483 mmol) yielded *rac*-**13c** (137.8 mg, 0.235 mmol, 49%) as lemon yellow prisms (9 h of refluxing in toluene and 1 h of refluxing in mesitylene). IR (Nujol, cm^{-1}): 2923 vs, 2854 vs, 2724 w, 1838 brm (ν(Si−H)), 1463 vs, 1417 w, 1377 s, 1348 w, 1339 w, 1302 m, 1270 m, 1249 s, 1209 w, 1152 m, 1033 sh, 1012 m, 954 brm, 892 w, 874 m, 836 m, 806 m, 778 m, 744 m, 721 w, 685 m, 647 w, 611 w, 570 w, 482 w, 462 w, 441 m, 420 m. ^{1}H NMR (400 MHz, C_6D_6, 25 °C): δ 7.78 (d, ^3J(H,H) = 8.2 Hz, 2 H, H7), 7.29 (d, ^3J(H,H) = 7.9 Hz, 2 H, H4), 6.79 (t, ^3J(H,H) = 7.6 Hz, 2 H, H6), 6.74 (t, ^3J(H,H) = 7.5 Hz, 2 H, H5), 6.13 (s, 2 H, H3), 3.74 (m, ^1J(Si,H) = 145 Hz, 2 H, SiH), 2.61 (s, 6 H, CH_3-indenyl), 1.05 (s, 6 H, Si(CH_3)$_2$), 0.06 (d, ^3J(H,H) = 2.5 Hz, 6 H, HSiCH_3(I)), −0.01 (d, ^3J(H,H) = 2.5 Hz, 6 H, HSiCH_3(II)). ^{13}C{^{1}H} NMR (100.5 MHz, C_6D_6, 25 °C): δ 136.1/133.5/133.2/124.0/121.8/ 121.4/121.0/107.1 (s, C2−C9), 104.3 (s, C1), 18.4 (s, *C*H_3-indenyl), 3.16 (s, HSi*C*H_3(I)), 2.29 (s, HSi*C*H_3(II)), 1.84 (s, *Si*CH_3). MS (CI): *m*/*z* (relative intensity) = 586 (54) [M^+], 453 (34) [M^+ − N(SiHMe$_2$)$_2$], 316 (47) [Me$_2$Si(Me-Ind)$_2^+$], 301 (24) [MeSi(Me-Ind)$_2^+$], 187 (100) [SiMe$_2$(Me-Ind)H$^+$], 132 (60) [N(SiHMe$_2$)$_2^+$], 118 (45) [N(SiHMe$_2$)(SiHMe)$^+$]. Anal. Calcd for $C_{26}H_{36}LaNSi_3$: C, 53.31; H, 6.19; N, 2.39. Found: C, 54.51; H, 6.50; N, 1.80.

***rac*-[Bis(dimethylsilyl)amido][η^5:η^5-bis(2-methylinden-1-yl)-dimethylsilyl]neodymium(III) (*rac*-13d).** Following the procedure described above, **7d** (701.0 mg, 1.023 mmol) and **3** (323.8 mg, 1.023 mmol) yielded *rac*-**13d** (266.4 mg, 0.451 mmol, 44%) as green prisms (12 h of refluxing in toluene and 2 h of refluxing in mesitylene). IR (Nujol, cm^{-1}): 2922 vs, 2853 vs, 2724 w, 1824 brm (ν(Si−H)), 1463 vs, 1409 w, 1377 s, 1344 w, 1332 w, 1302 m, 1267 m, 1246 s, 1198 w, 1150 m, 1029 sh, 1000 m, 975 brm, 937 sh m, 898 w, 873 m, 833 m, 806 m, 791 w, 776 m, 748 m, 721 w, 686 m, 652 w, 643 w, 612 w, 570 w, 483 w, 462 w, 445 m, 420 m. ^{1}H NMR (400 MHz, C_6D_6, 20.6 °C): δ 23.6 (s, 6 H, lw = 105 Hz), 13.7 (s, 6 H, lw = 46 Hz), 11.5 (s, 6 H, lw = 45 Hz), 2.2 (s, 2 H, lw = 5 Hz), −0.4 (s, 2 H, lw = 186 Hz), −2.1 (s, 2 H, lw = 60 Hz), −11.1 (s, 6 H, lw = 304 Hz), −13.4 (s, 2 H, lw = 34 Hz), −21.7 (s, 2 H, lw = 91 Hz); a Si−H signal could not be detected. MS (CI): *m*/*z* (relative intensity) 591 (55) [M^+], 458 (30 [M^+ − N(SiHMe$_2$)$_2$], 316 (47) [SiMe$_2$(Me-Ind)$_2$H$^+$], 301 (25) [MeSi(Me-Ind)$_2^+$], 187 (100) [SiMe$_2$(Me-Ind)H$^+$], 132 (55) [N(SiHMe$_2$)$_2^+$], 118 (49) [N(SiHMe$_2$)(SiHMe)$^+$]. Anal. Calcd for $C_{26}H_{36}NNdSi_3$: C, 52.83; H, 6.14; N, 2.37. Found: C, 52.11; H, 6.50; N, 2.30.

***rac*-[Bis(dimethylsilyl)amido][η^5:η^5-bis(2-methylinden-1-yl)dimethylsilyl]lutetium(III) (*rac*-13e).** Following the procedure described above, **7e** (716.2 mg, 1.000 mmol) and **3** (316.5 mg, 1.000 mmol) yielded *rac*-**13e** (201.5 mg, 0.324 mmol, 32%) as lemon yellow prisms (24 h of refluxing in toluene and 24 h of refluxing in mesitylene). IR (Nujol, cm^{-1}): 2922 vs, 2853 vs, 2723 m, 1759 brw (ν(Si−H)), 1463 vs, 1409 w, 1377 s, 1341 m, 1335 m, 1269 m, 1245 s, 1150 w, 1086 sh, 1035 m, 997 w, 901 m, 833 m, 807 m, 783 s, 764 m, 746 s, 690 m, 658 w, 657 w, 644 m, 612 w, 570 w, 484 w, 448 s, 428 m. ^{1}H NMR (400 MHz, C_6D_6, 25 °C): δ 7.84 (d, ^3J(H,H) = 8.4 Hz, 2 H, H7), 7.42 (d, ^3J(H,H) = 8.0 Hz, 2 H, H4), 6.90 (dd, 2× ^3J(H,H) = 7.7 Hz, 2 H, H6), 6.83 (dd, 2× ^3J(H,H) = 7.3 Hz, 2 H, H5), 6.19 (s, 2 H, H3), 3.29 (sept, ^1J(Si,H) = 146 Hz, ^3J(H,H) = 2.6 Hz, 2 H, SiH), 2.39 (s, 6 H, CH_3-indenyl), 1.10 (s, 6 H, Si(CH_3)$_2$), 0.10 (d, ^3J(H,H) = 2.6 Hz, 6 H, HSiCH_3(I)), 0.07 (d, ^3J(H,H) = 2.6 Hz, 6 H, HSiCH_3(II)). ^{13}C{^{1}H} NMR (100.5 MHz, C_6D_6, 25 °C): δ 136.6/130.8/130.2/123.7/123.5/122.1/121.9/108.1 (s, C2−C9), 98.2 (s, C1), 17.91 (s, *C*H_3-indenyl-(I)), 17.89 (s, *C*H_3-indenyl(II)), 3.06 (s, HSi*C*H_3), 2.78 (s, Si*C*H_3). MS (CI): *m*/*z* (relative intensity) 621 (100) [M^+ − H], 605 (18) [M^+ − CH_3 − 2H], 562 (4) [M^+ − SiHMe$_2$], 389 (10) [M^+ − N(SiHMe$_2$)$_2$], 316 (8) [SiMe$_2$(Me-Ind)$_2$H$^+$], 310 (13) [SiMe$_2$(Me-Ind)$_2^+$ − CH_3], 187 (27) [SiMe$_2$(Me-Ind)H$^+$], 132 (7) [N(SiHMe$_2$)$_2^+$]. Anal. Calcd for $C_{26}H_{36}LuNSi_3$: C, 50.22; H, 5.84; N, 2.26. Found: C, 50,12; H, 6.38; N, 1.96.

Bis[bis(dimethylsilyl)amido][η^5-bis(2-methyl-4-phenylinden-1-yl)-dimethylsilyl]yttrium(III) (14b). Following the procedure described above, **7b** (630.1 mg, 1.000 mmol) and **4** (468.8 mg, 1.000 mmol) yielded **14b** (90.3 mg, 0.065 mmol, 11%) as lemon yellow prisms (24 h of refluxing in toluene and 10 h of refluxing in mesitylene). IR (Nujol, cm^{-1}): 2923 vs, 2853 vs, 2723 w, 2069 m, 1830 brw (ν(Si−H)), 1462 vs, 1610 w, 1410 w, 1379 s, 1344 m, 1333 m, 1279 m, 1246 s, 1150 m, 1037 m, 1000 m, 902 m, 876 s, 833 s, 807 s, 781 s, 765 s, 748 s, 690 m, 656 w, 644 m, 611 w, 571 w, 484 w, 460m, 449 s, 429 m. ^{1}H NMR (400 MHz, C_6D_6, 25 °C): δ 7.88 (dd, ^3J(H,H) = 8.4 Hz, ^4J(H,H) = 1.3 Hz, 2 H, phenyl(I)), 7.84 (d, ^3J(H,H) = 8.4 Hz, 1 H), 7.57 (dd, ^3J(H,H) = 8.4 Hz, ^4J(H,H) = 1.3 Hz, 2 H, phenyl(II)), 7.35−7.23 (m, 4 H, phenyl + indenyl), 7.19−7.11 (m, 5 H, phenyl), 7.02 (dd, 2× ^3J(H,H) = 7.5 Hz, 1 H), 6.94 (s, 1H, indenyl), 6.82 (s, 1 H, indenyl), 6.58 (d, ^3J(H,H) = 8.0 Hz, 1 H), 4.31 (dsept, ^1J(Si,H) = 148 Hz, ^3J(H,H) = 2.9 Hz, 4 H, SiH), 3.66 (s, 1 H, indenyl), 2.34 (s, 3 H, CH_3-indenyl(I)), 1.75 (s, 3 H, CH_3-indenyl(II)), 0.67 (s, 3 H, Si(CH_3)$_2$-(I)), 0.48 (s, 3 H, Si(CH_3)$_2$(II)), 0.12 (d, ^3J(H,H) = 2.5 Hz, 24 H, HSi-(CH_3)$_2$). ^{13}C{^{1}H} NMR (100.5 MHz, C_6D_6, 25 °C): δ 162.9/148.0/145.8/145.2/143.0/142.0/140.9/137.7/137.4/134.1/130.1/129.8/128.4/127.9/127.2/126.6/125.6/125.4/123.2/123.1/123.0/122.8/122.2/122.1/105.8 (s, phenyl + indenyl), 49.9 (s, indenyl-C3), 18.0 (s, *C*H_3-indenyl(I)), 16.9 (s, *C*H_3-indenyl(I)), 2.56 (s, HSi*C*H_3(I)), 2.42 (s, HSi*C*H_3(II)), 0.58 (s, Si(*C*H_3)$_2$(I)), −0.69 (s, Si(*C*H_3)$_2$(II)). MS (CI): *m*/*z* (relative intensity) 821 (3) [M^+], 689 (5) [M^+ − N(SiHMe$_2$)$_2$], 557 (45) [M^+ − 2N(SiHMe$_2$)$_2$], 468 (54) [Me$_2$Si(2-Me-4-Ph-Ind)$_2$H$^+$], 263 (100) [Me$_2$Si(2-Me-4-Ph-Ind)H$^+$], 132 (20) [N(SiHMe$_2$)$_2^+$]. Anal. Calcd for $C_{42}H_{59}YN_2Si_5$: C, 61.43; H, 7.24; N, 3.41. Found: C, 59.94; H, 7.09; N, 3.16.

***rac*-[Bis(dimethylsilyl)amido][η^5:η^5-bis(2-methyl-4-phenylinden-1-yl)dimethylsilyl]lanthanum(III) (*rac*-14c).** Following the procedure described above, **7c** (340.1 mg, 0.500 mmol) and **4** (234.4 mg, 0.500 mmol) yielded *rac*-**14c** (48.0 mg, 0.065 mmol, 13%) as lemon yellow needles (24 h of refluxing in toluene and 5 h of refluxing in mesitylene). IR (Nujol, cm^{-1}): 2923 vs, 2853 vs, 2723 w, 1832 brw (ν(Si−H)), 1462 vs, 1610 w, 1410 w, 1379 s, 1344 m, 1333 m, 1279 m, 1246 s, 1150 m, 1037 m, 1000 m, 902 m, 876 s, 833 s, 807 s, 781 s, 765 s, 748 s, 690 m, 656 w, 644 m, 611 w, 571 w, 484 w, 460 m, 449 s, 429 m. ^{1}H NMR (400 MHz, C_6D_6, 25 °C): δ 7.84 (d, ^3J(H,H) = 8.4 Hz, 2 H, H7), 7.42 (d, ^3J(H,H) = 8.0 Hz, 2 H, H5), 7.35−7.25 (m, 12 H, phenyl), 6.89 (dd, 2× ^3J(H,H) = 7.7 Hz, 2 H, H6), 6.59 (s, 2 H, H3), 3.87 (m, ^1J(Si,H) = 141 Hz, 2 H, SiH), 2.58 (s, 6 H, CH_3-indenyl), 1.11 (s, 6 H, Si(CH_3)$_2$), −0.14 (d, ^3J(H,H) = 2.5 Hz, 6 H, HSi(CH_3)$_2$-(I)), −0.29 (d, ^3J(H,H) = 2.5 Hz, 6 H, HSi(CH_3)$_2$(II)). ^{13}C{^{1}H} NMR (100.5 MHz, C_6D_6, 25 °C): δ 141.0/136.3/135.3/131.9/129.3/128.9/127.5/127.2/123.1/121.3/120.5/108.4/100.6 (s, phenyl + indenyl), 18.2 (s, *C*H_3-indenyl), 3.22 (s, Si(*C*H_3)$_2$), 2.10 (s, HSi*C*H_3(I)), 1.95 (s, HSi*C*H_3(II)). MS (CI): *m*/*z* (relative intensity) 738 (9) [M^+], 468 (54) [Me$_2$Si(2-Me-4-Ph-Ind)$_2$H$^+$], 263 (100) [Me$_2$Si(2-Me-4-Ph-Ind)H$^+$], 132 (20) [N(SiHMe$_2$)$_2^+$]. Anal. Calcd for $C_{38}H_{44}LaNSi_3$: C, 61.85; H, 6.01; N, 1.90. Found: C, 61.47; H, 6.12; N, 1.75.

***rac*-[Bis(dimethylsilyl)amido][η^5:η^5-bis(2-methyl-4,5-benzoinden-1-yl)dimethylsilyl]yttrium(III) (*rac*-15b).** Following the procedure described above, **7b** (630.1 mg, 1.000 mmol) and **5** (416.7 mg, 1.000 mmol) yielded *rac*-**15b** (459.7 mg, 0.723 mmol, 72%) as light yellow prisms (18 h of refluxing in toluene and 13 h of refluxing in mesitylene). IR (Nujol, cm^{-1}): 2922 vs, 2853 vs, 2724 m, 1811 brw (ν(Si−H)), 1608 w, 1462 vs, 1376 s, 1351 m, 1277 w, 1247 m, 1241 m, 1172 brs, 1096 w, 1027 m, 973 m, 938 w, 902 m, 896 w, 868 w, 836 w, 814 w, 800 m, 766 s, 727 s, 682 m, 644 m, 467 m, 431 m. ^{1}H NMR (400 MHz, C_6D_6, 25 °C): δ 7.95 (d, ^3J(H,H) = 7.4 Hz, 2 H, H7), 7.93 (d, ^3J(H,H) = 7.4 Hz, 2 H, H6), 7.61 (dd, ^3J(H,H) = 7.7 Hz, ^4J(H,H) = 1.3 Hz, 2 H, benzo-H), 7.27−7.18 (m, 6 H, benzo-H), 6.72 (s, 2 H, H3), 2.65 (dsept, J(Y,H) = 4.8 Hz, ^1J(Si,H) = 133 Hz, ^3J(H,H) = 2.5 Hz, 2 H, SiH), 2.56 (s, 6 H, CH_3-indenyl), 1.15 (s, 6 H, Si(CH_3)$_2$), −0.03 (d, ^3J(H,H) = 2.5 Hz, 6 H, HSiCH_3(I)), −0.87 (d, ^3J(H,H) = 2.5 Hz, 6 H, HSiCH_3(II)). ^{13}C{^{1}H} NMR (100.5 MHz, C_6D_6, 25 °C): δ 133.7/130.6/129.6/129.3/128.9/127.0/126.7/125.2/124.0/123.3/123.2/109.4/104.0 (s, *C*-benzoindenyl), 18.2 (s, *C*H_3-indenyl), 3.07 (s, Si*C*H_3), 2.89 (s, HSi*C*H_3(I)), −0.10 (s, HSi*C*H_3(II)). ^{29}Si{^{1}H} NMR (79.5 MHz, C_6D_6, 25 °C): δ −15.90 (d, ^1J(Y,Si) = 1.2 Hz, Si_{bridge}), −26.61 (d, ^1J(Y,Si) = 12.2 Hz, NSi). ^{89}Y NMR (19.48 MHz, toluene/C_6D_6, 30 °C): δ −93.5 (t, ^1J(Y,H) = 4.7 Hz). MS (CI): *m*/*z* (relative intensity) 651 (31) [M^+ + CH_3], 636 (31) [M^+], 635 (60) [M^+ − H], 621 (11) [M^+ − CH_3], 503 (28) [M^+ − N(SiHMe$_2$)$_2$], 416 (58) [SiMe$_2$(Me-

Table 5. X-ray Diffraction Collection Parameters for Organolanthanide Complexes

	11c	*rac*-**13b**	*rac*-**13e**	*rac*-**15b**	*rac*-**15e**
formula	$C_{24}H_{44}LaNSi_3$	$C_{26}H_{36}YNSi_3$	$C_{26}H_{36}LuNSi_3$	$C_{34}H_{40}YNSi_3 \cdot (C_7H_8)_{0.5}$	$C_{34}H_{40}LuNSi_3$
formula weight	569.78	535.74	621.80	635.86·46.07	721.91
crystal system	triclinic	monoclinic	monoclinic	triclinic	triclinic
space group	$P\bar{1}$	$C2/c$	$C2/c$	$P\bar{1}$	$P\bar{1}$
a/Å	9.529(1)	15.110(4)	15.0153(4)	11.1193(6)	11.6187(7)
b/Å	11.145(1)	11.731(2)	11.8938(5)	11.9449(5)	12.1293(8)
c/Å	13.573(1)	15.699(5)	15.7695(5)	14.8399(8)	13.9320(11)
α/deg	79.68(1)	90	90	72.396(5)	78.198(8)
β/deg	83.26(1)	108.55(1)	108.145(2)	75.824(6)	67.611(8)
γ/deg	77.61(1)	90	90	69.896(5)	63.935(7)
V/Å^3	1380.4(2)	2638.2(12)	2676.21(16)	1742.2(2)	1629.1(2)
Z	2	4	4	2	2
ρ_{calcd}/g cm^{-1}	1.371	1.349	1.543	1.300	1.472
μ/cm^{-1}	16.9	23.6	38.4	18.0	31.6
F(000)	588	1120	1248	714	728
temperature/K	193	163	273	193	293
λ(Mo Kα)/Å	0.710 73	0.710 73	0.710 73	0.710 73	0.710 73
diffractometer	STOE-IPDS	Nonius-CAD4	Nonius-κCCD	STOE-IPDS	STOE-IPDS
scan type	φ scans	ω scans	φ scans	φ scans	φ scans
θ range/deg	1.9−24.7	2.2−26.0	4.9−25.4	2.0−24.7	3.1−25.7
no. of total/unique data	12166/4365	4534/2472	4071/2203	21813/5536	9550/5683
no. of observed data	3986	2147	2085	4525	4486
no of parameters	396	214	214	373	365
H atoms	refined	refined	refined	mixed	calcd
final $R1$[a]	0.0291/0.0247	0.0403/0.0318	0.0223/0.0206	0.0463/0.0358	0.0459/0.0332
final w$R2$[b]	0.0605	0.0742	0.0474	0.0944	0.769
GOF	1.037	1.048	1.094	0.973	0.916
difference Fourier	0.91/−1.01	0.52/−0.45	0.27/−0.79	0.98/−0.45	0.74/−0.51

[a] $R1 = \sum(||F_o| - |F_c||)/\sum|F_o|$. [b] $wR2 = [\sum w(|F_o^2 - F_c^2|^2)/wF_o^2]^{1/2}$

Benz-Ind)$_2$H$^+$], 237 (100) [SiMe$_2$(Me-Benz-Ind)H$^+$], 221 (7) [YN(SiHMe$_2$)$_2^+$], 180 (10) [(Me-Benz-Ind)H$^+$], 132 (13) [N(SiHMe$_2$)$_2^+$], 118 (17) [N(SiHMe$_2$)$_2^+$ − CH$_3$]. Anal. Calcd for $C_{34}H_{40}NSi_3Y$: C, 64.22; H, 6.34; N, 2.20. Found: C, 63.58; H, 6.37; N, 2.04. Recrystallization of *rac*-**15b** from toluene results in incorporation of solvent into the crystal. Anal. Calcd for $C_{34}H_{40}NSi_3Y \cdot C_7H_8$: C, 67.64; H, 6.64; N, 1.94. Found: C, 66.54; H, 6.50; N, 1.94.

***rac*-[Bis(dimethylsilyl)amido][η^5:η^5-bis(2-methyl-4,5-benzoinden-1-yl)dimethylsilyl]lanthanum(III) (*rac*-15c).** Following the procedure described above, **7c** (680.1 mg, 1.000 mmol) and **5** (416.7 mg, 1.000 mmol) yielded *rac*-**15c** (320.3 mg, 0.467 mmol, 47%) as light yellow prisms (18 h of refluxing in toluene and 6 h of refluxing in mesitylene). IR (Nujol, cm^{-1}): 2923 vs, 2853 vs, 2723 w, 1830 brw (ν(Si−H)), 1610 w, 1462 vs, 1377 s, 1352 m, 1279 w, 1250 m, 1214 w, 1155 brs, 1096 w, 1027 m, 997 w, 974 m, 938 w, 897 m, 873 m, 834 m, 812 m, 800 m, 765 s, 724 w, 679 m, 645 w, 466 m, 432 m. ^{1}H NMR (400 MHz, C$_6$D$_6$, 25 °C): δ 7.90 (d, ^3J(H,H) = 7.4 Hz, 2 H, H7), 7.86 (d, ^3J(H,H) = 7.4 Hz, 2 H, H6), 7.61 (dd, ^3J(H,H) = 7.4 Hz, ^4J(H,H) = 1.1 Hz, 2 H, benzo-H), 7.25−7.17 (m, 6 H, benzo-H), 6.72 (s, 2 H, H3), 3.30 (m, ^1J(Si,H) = 140 Hz, 2 H, SiH), 2.53 (s, 6 H, CH_3-indenyl), 1.15 (s, 6 H, Si(CH_3)$_2$), −0.087 (d, ^3J(H,H) = 2.5 Hz, 6 H, HSiCH_3(I)), −0.81 (d, ^3J(H,H) = 2.5 Hz, 6 H, HSiCH_3(II)). ^{13}C{^{1}H} NMR (100.5 MHz, C$_6$D$_6$, 25 °C): δ 133.2/131.9/129.9/129.0/128.7/127.1/126.6/124.7/123.2/123.1/122.0/108.7/104.7 (s, *C*-benzoindenyl), 17.8 (s, *C*H$_3$-indenyl), 3.12 (s, SiCH$_3$), 1.91 (s, HSi*C*H$_3$(I)), −0.18 (s, HSi*C*H$_3$(II)). MS (CI): *m*/*z* (relative intensity) 686 (23) [M$^+$], 685 (42) [M$^+$ − H], 671 (14) [M$^+$ − CH$_3$], 553 (33) [M$^+$ − N(SiHMe$_2$)$_2$], 416 (73) [SiMe$_2$(Me-Benz-Ind)$_2$H$^+$], 237 (100) [SiMe$_2$(Me-Benz-Ind)H$^+$], 180 (22) [(Me-Benz-Ind)H$^+$], 132 (19) [N(SiHMe$_2$)$_2^+$], 118 (11) [N(SiHMe$_2$)$_2^+$ − CH$_3$]. Anal. Calcd for $C_{34}H_{40}LaNSi_3$: C, 59.54; H, 5.88; N, 2.04. Found: C, 59.39; H, 6.14; N, 1.91.

***rac*-[Bis(dimethylsilyl)amido][η^5:η^5-bis(2-methyl-4,5-benzoinden-1-yl)dimethylsilyl]lutetium(III) (*rac*-15e).** Following the procedure described above, **7e** (1343.7 mg, 1.897 mmol) and **5** (790.5 mg, 1.897 mmol) yielded *rac*-**15e** (743.6 mg, 1.030 mmol, 54%) as light yellow prisms (18 h of refluxing in toluene and 12 h of refluxing in mesitylene). IR (Nujol, cm^{-1}): 2922 vs, 2853 vs, 2725 w, 1773 brw (ν(Si−H)), 1611 w, 1463 vs, 1377 s, 1351 m, 1276 w, 1249 w, 1238 m, 1162 m, 1138 w, 1095 w, 1080 w, 1041 m, 1027 m, 991 shm, 895 w, 857 w, 834 w, 811 m, 800 m, 766 m, 741 m, 722 m, 683 m, 644 w, 467 m, 431 w. ^{1}H NMR (400 MHz, C$_6$D$_6$, 25 °C): δ 7.97 (d, ^3J(H,H) = 7.6 Hz, 2 H, H7), 7.89 (d, ^3J(H,H) = 9.0 Hz, 2 H, H6), 7.60 (dd, ^3J(H,H) = 7.9 Hz, ^4J(H,H) = 1.0 Hz, 2 H, benzo-H), 7.29−7.19 (m, 6 H, benzo-H), 6.75 (s, 2 H, H3), 2.98 (sept, ^1J(Si,H) = 142 Hz, ^3J(H,H) = 2.5 Hz, 2 H, SiH), 2.52 (s, 6 H, CH_3-indenyl), 1.14 (s, 6 H, Si(CH$_3$)$_2$), −0.055 (d, ^3J(H,H) = 2.5 Hz, 6 H, HSiCH_3(I)), −0.77 (d, ^3J(H,H) = 2.5 Hz, 6 H, HSiCH_3(II)). ^{13}C{^{1}H} NMR (100.5 MHz, C$_6$D$_6$, 25 °C): δ 132.5/130.7/129.7/128.8/126.9/126.1/125.3/124.6/124.3/123.4/123.2/109.3/103.4 (s, *C*-benzoindenyl), 18.0 (s, *C*H$_3$-indenyl), 3.52 (s, SiCH$_3$), 2.98 (s, HSi*C*H$_3$(I)), 0.26 (s, HSi*C*H$_3$(II)). MS (CI): *m*/*z* (relative intensity) 721 (37) [M$^+$], 620 (68) [M$^+$ − H], 706 (20) [M$^+$ − CH$_3$], 588 (41) [M$^+$ − N(SiHMe$_2$)$_2$], 416 (45) [SiMe$_2$(Me-Benz-Ind)$_2$H$^+$], 237 (100) [SiMe$_2$(Me-Benz-Ind)H$^+$], 180 (17) [(Me-Benz-Ind)H$^+$], 132 (14) [N(SiHMe$_2$)$_2^+$], 118 (21) [N(SiHMe$_2$)$_2^+$ − CH$_3$]. Anal. Calcd for $C_{34}H_{40}NSi_3Lu$: C, 56.67; H, 5.58; N, 1.94. Found: C, 66.38; H, 5.69; N, 1.82.

[Bis(dimethylsilyl)amido][η^5:η^5-bisfluoren-9-yl-dimethylsilyl]-yttrium(III) (16b). Following the procedure described above, **7b** (945.0 mg, 1.500 mmol) and **6** (583.0 mg, 1.500 mmol) yielded 174 mg of an orange powder (24 h of refluxing in toluene and 5 h of refluxing in mesitylene). According to NMR spectroscopy, this powder contained about 35% of **16b** in addition to unreacted bis(fluorene) and a complex containing a monocoordinated bis(fluorene). ^{1}H NMR (400 MHz, C$_6$D$_6$, 25 °C): δ 8.11 (d, ^3J(H,H) = 8.1 Hz, 4 H, fluorene-H), 8.08 (d, ^3J(H,H) = 8.3 Hz, 4 H, fluorene-H), 7.21 (t, ^3J(H,H) = 7.4 Hz, 4 H, fluorene-H), 6.85 (t, ^3J(H,H) = 7.2 Hz, 4 H, fluorene-H), 3.21 (sept, ^3J(H,H) = 2.5 Hz, 2 H, SiH), 0.96 (s, 6 H, Si(CH_3)$_2$), −0.13 (d, ^3J(H,H) = 2.6 Hz, 12 H, HSi(CH_3)$_2$).

(Tetrahydrofurano)tris[bis(dimethylsilyl)amido]yttrium(III) (17b). In a glovebox, **7b** (630 mg, 1.00 mmol) was placed in a 100-mL flask with fused reflux condenser, dissolved in 20 mL of toluene, and refluxed under a slight argon purge for 12 h. Then the solvent was removed in vacuo, and the residue was dried at 10^{-4} mbar, producing **17b** as a white powder (512 mg, 0.92 mmol, 92%). IR (Nujol, cm^{-1}): 2924 vs, 2854 vs, 2724 m, 2067 s, 1931 (sh) m (ν(Si−H)), 1462 vs, 1377 s, 1247 s, 1040 brvs, 897 vs, 837 s, 789 m, 784 m, 684 w, 609 w, 406 w. ^{1}H NMR (400 MHz, C$_6$D$_6$, 25 °C): δ 4.94 (sept, ^1J(Si,H) = 162 Hz, ^3J(H,H) = 2.96 Hz, 6 H, SiH), 3.75 (brs, 4 H, THF(I)), 1.21 (m, 4 H, THF(II)), 0.37 (d, ^3J(H,H) = 3.0 Hz, 36 H, SiCH$_3$). ^{13}C{^{1}H} NMR

(100.5 MHz, C_6D_6, 25 °C): δ 70.6 (s, THF), 24.2 (s, THF), 2.30 (s, $SiCH_3$). $^{29}Si\{^1H\}$ NMR (79.5 MHz, C_6D_6, 25 °C): δ −22.39 (s). MS (CI): *m*/*z* (relative intensity) = 778 (13) [$M^+ + Y\{N(SiMe_2H)_2\}$], 557 (2) [$M^+ - H$], 484 (44) [$M^+ - THF + H$], 470 (58) [$M^+ - THF - CH_3$], 426 (100) [$M^+ - N(SiMe_2H)_2$], 353 (36) [$M^+ - THF - N(SiMe_2H)_2$], 293 (69) [$M^+ - 2N(SiMe_2H)_2$], 132 (58) [$N(SiMe_2H)_2^+$], 118 (93) [$HN(HSiMe_2)(SiHMe)^+$]. Anal. Calcd for $C_{16}H_{50}YN_3OSi_6$: C, 34.41; H, 9.03; N, 7.53. Found: C, 34.64; H, 8.80; N, 6.36.

X-ray Data Collection and Refinement. Single crystals of the complexes **11c**, *rac*-**13b**, *rac*-**13e**, *rac*-**15b**, and *rac*-**15e** were grown at −35 °C from toluene/*n*-hexane solutions. The X-ray diffraction data were collected on a Nonius CAD-4 diffractometer[76] for complex *rac*-**13b**, on a Nonius Kappa-CCD-system[76] for *rac*-**13e**, and on a STOE-IPDS[77] for **11c**, *rac*-**15b**, and *rac*-**15e**.

Preliminary positions of heavy atoms were found by direct methods,[78] while positions of the other non-hydrogen atoms were determined from successive Fourier difference maps coupled with initial isotropic least-squares refinement.[79] All of the non-hydrogen positions were refined anisotropically. For *rac*-**15b,** the difference Fourier synthesis showed several electron density peaks in the vicinity of the symmetry center. These peaks correspond to a disordered toluene solvate molecule. The final least-squares refinement was performed using anisotropic thermal parameters for the non-hydrogen atoms of the metal complex and isotropic thermal parameters for the atoms of the solvate molecule. Hydrogen atoms were located from difference Fourier maps and refined for **11c**, *rac*-**13b**, and *rac*-**13e**, refined only for Si−H in the case of *rac*-**15b**, and placed in calculated positions for *rac*-**15e**. All details of the data collection and the crystal and refinement parameters are summarized in Table 5.

Acknowledgment. We thank the Deutsche Forschungsgemeinschaft for the award of a DFG fellowship to R.A.

Supporting Information Available: Tables of crystal data, structure solution and refinement, atomic coordinates, bond lengths and angles, and anisotropic thermal parameters for **11c**, *rac*-**13b**, *rac*-**13e**, *rac*-**15b**, and *rac*-**15e** (PDF). X-ray crystallographic data, in CIF format, are also available. This material is available free of charge via the Internet at http://pubs.acs.org.

JA992786A

(76) Otwinowski, Z.; Minov, W. In *Methods in Enzymology*; Caster, C. W., Jr., Sweet, R. M., Eds.; Academic Press: New York, 1996; Vol. 276.

(77) *IPDS Operating System*, Version 2.6; STOE&CIE.GMBH: Darmstadt, Germany, 1995.

(78) Altomare, A.; Cascarano, G.; Giacovazzo, C.; Guagliardi, A. *J. Appl. Crystallogr.* **1998**, *26*, 343−350.

(79) Sheldrick, G. M. *SHELXL 93*; Universität Göttingen, Germany, 1993.

(80) Spek, A. L. *Acta Crystallogr. A* **1990**, *46*, C-34.